ChemE 6681

Energy Analysis Project

James Hayes and Reynold Gao

Topic: Evaluation of the potential of Compressed Air Energy Storage (CAES) to meet peak power demands in NY State using underground salt deposits located in the Finger Lake region of central NY

Objectives: To assess the principles and the state of CAES technology, to determine the feasibility of CAES with Finger Lakes salt deposits, to evaluate the ability of CAES to meet peak NYS power demands, or to supplement it. To explore the practical considerations in implementing CAES. To compare CAES with alternative storage options.

Approach: We introduce CAES and its various types. Then we analyze the technology used in a CAES facility and simulate a simple example of A-CAES. Next, we discuss the specifics of the Finger Lakes salt mines and any safety, environmental, and regulatory concerns. Then we consider New York's energy needs and provide recommendations for implementing a CAES facility.

TABLE OF CONTENTS

Introduction to CAES

Variable renewable energy resources in the U.S., such as wind and solar, are projected to scale up dramatically in the coming years, according to the EIA[1]. New York State (NYS) in particular has ambitious goals for solar and offshore wind. 6,000 MW of solar and 9,000 MW of offshore wind are planned by 2025 and 2035, respectively[2]. Due to their short term and seasonal variability, these technologies are limited in their dispatchability, meaning that during certain periods they may overgenerate power or produce very little. Consequently, in order to meet peak load requirements, the upcoming increase in variable renewable generation will also grow the need for energy storage technologies. One such method is called Compressed Air Energy Storage (CAES).

This technology stores electrical energy by using it to power a gas compressor which pressurizes ambient air. The compressed air can then be stored, usually in an underground cavern. When energy needs to be recovered, the stored air can be run through a turbine and de-pressurized, thus producing electricity.

CAES has several advantages which make it an attractive choice for energy storage[3,4,5]. It is capable of storing energy for long periods of time relative to other methods, on the order of days to years. CAES also generally has a high energy storage capacity and power output. Furthermore, compressors, turbines, and mining equipment often used in the oil and gas industry is easily available and can be repurposed for use in a CAES facility.

New York State has set a goal for 3,000 MW of energy storage by 2030. CAES technology offers an excellent opportunity to meet this target due to its relatively low cost and high power and energy capacity. Furthermore, the Finger Lakes region of central NY presents ideal geology for a CAES facility, specifically the salt mines on Cayuga and Seneca Lakes.

In this paper, we will examine the types of CAES, the state of the technology, and its principles. A basic analysis using the ideal gas law will be discussed, alongside a more thorough process simulation. We will also explore the Finger Lake salt mines as a storage vessel for CAES and NYS energy storage needs. Finally, an economic comparison will be presented to highlight why CAES may be a good choice for energy storage in NYS.

Types of CAES

CAES systems can be classified into three different types. They are generally defined based on how or if the air is reheated before expansion.

The first type of CAES process to be implemented is called diabatic (D-CAES). It is defined by the re-heating of air prior to expansion in the turbine using an external energy source[6,7]. Natural gas combustion is typically used for this. Unfortunately, even the most advanced natural gas combustion cycles have limited efficiencies. Moreover, there are significant losses to the cooling of air after compression. Therefore, D-CAES is characterized by rather low efficiencies around 40-55%. D-CAES also is not emission free, making it a less attractive choice given the increasing focus on renewable and sustainable energy.

Adiabatic CAES (A-CAES) does not require any fossil fuel combustion for air re-heating. Instead, heat produced during compression is used to re-heat the air before it is expanded. A-CAES utilizes thermal energy storage systems to store the recovered heat from the compressed gas[6,7]. Possible thermal energy storage methods can include hot water, phase change materials, or molten salt. When electricity needs to be generated from the A-CAES process, the stored thermal energy is released to re-heat the turbine inlet air. By avoiding external heating and significant heat losses to the environment, A-CAES can have an efficiency ranging from 60% to 70% or more.

There is one type of CAES which does not involve re-heating air at all. It is called isothermal/near-isothermal CAES (I-CAES). This process includes both isothermal compression and expansion, which is accomplished by rapid heat exchange with the environment during the pressure change[8]. This allows for very good efficiencies, in the range of 90-95%. Theoretically, a perfectly isothermal system would have an efficiency of 100%. However, near-isothermal systems have one serious disadvantage. Limitations in heat exchangers prevent isothermal CAES from being practical for high air flow rates and power levels. Heat simply cannot be removed fast enough for such larger scale systems.

History of CAES and Existing Facilities

Although there are currently very few CAES facilities in the world, the concept of using compressed air as a power source is not a new one. Compressed air has been used to power machinery, tools, and generators since the 19th century. For example, in 1888, engineer Viktor Popp created a compressed air plant in Paris, France which had an initial capacity of 1.5 MW, later improved to a capacity of 18 MW[9], which was rather impressive for the time.

It was not until the 20th century that compressed air's potential for utility-scale energy storage was investigated and realized. In 1949, a CAES process involving underground storage was

patented for the first time in the US[10]. Despite this early investigation and testing of CAES, it would still be many years until the technology was adopted for practical commercial applications.

The first commercial CAES facility was commissioned in Huntorf, Germany in 1978. This facility uses a D-CAES process[11]. It makes use of two salt domes that are about 650-800 m underground for storing the compressed air. A third cavern is used to store the natural gas needed to reheat the air.

The second utility scale CAES facility was constructed in McIntosh, Alabama in 1991. PowerSouth Energy Cooperative owns this facility. Like the Huntorf facility in Germany, the McIntosh facility is a diabatic CAES project. It also uses a single salt cavern for storage of the compressed air, which is about 450 m below ground[12,13]. Some of the data for these two facilities is displayed in Table 1.

Table 1. Specifications of Huntorf and McIntosh CAES facilities[11,14].

Data	Huntorf CAES	McIntosh CAES
Nameplate power capacity (MW)	290	110
Energy capacity (MWh)	580	2,860
Efficiency (%)	42	54
Storage Volume (m^3)	310,000	560,000
Pressure (bar)	43-70	45-74
Turbine mass flow rate (kg/s)	416	154
Compressor mass flow rate (kg/s)	104	96
Compressor rated power (MW)	62	53
Start up time to full load (min)	11	14

Being both D-CAES, the processes in these two facilities are rather similar. The process flow diagrams of the Huntorf and McIntosh facilities are depicted in Figures 1 and 2, respectively[15,16].

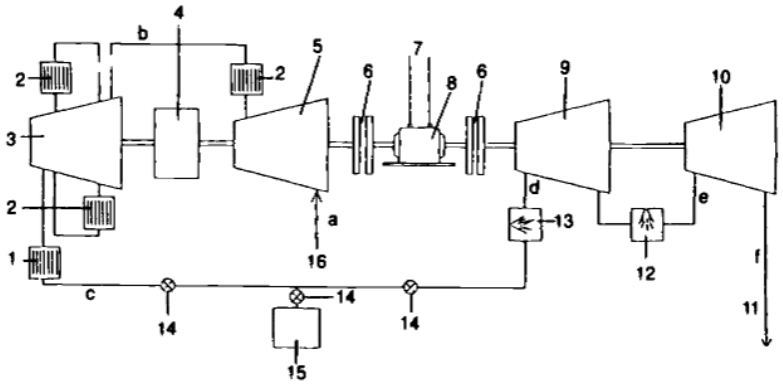

Fig. 7.9 Huntorf CAES

		Power conditions
1	aftercooler	*a* - 15°C, 1 bar
2	intercooler	*b* - 55 bar
3	compressor (high pressure stage)	*c* - 37°C, 68 bar
4	gear box	*d* - 550°C, 43 bar
5	compressor (low pressure stage)	*e* - 825°C, 11 bar
6	clutch	*f* - 390°C, 11 bar
7	transmission line	
8	motor/generator	
9	high pressure turbine	
10	low pressure turbine	
11	exhaust	
12	low pressure combustor chamber	
13	high pressure combustor chamber	
14	valve	
15	air cavity	
16	intake	

Figure 1. Process Flow Diagram of Huntorf CAES facility[15].

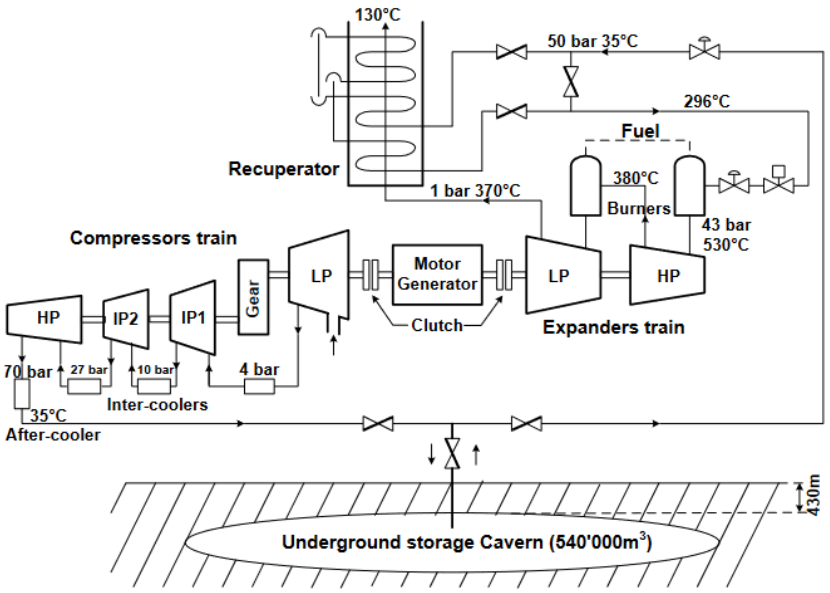

Figure 2. Process Flow Diagram of McIntosh CAES facility[16].

The Huntorf and McIntosh process flow diagrams share the same general layout. Both have several compressors per train and intercoolers between each. There are also two turbines per train with natural gas burners before each. Their cavern outlet pressures are also quite similar (50 vs 55 bar). This reflects some loss in air pressure during storage for both facilities. This loss is most likely due to cooling of the air during storage rather than significant leakage.

The data on the two CAES facilities show that they both store energy at a rate much slower than it can be discharged. It is about a factor of 4 slower for the Huntorf facility and 1.6 for the McIntosh facility (Table 1). This feature is acceptable for peak shaving applications since it allows for high output during peak demand for short durations but generally allows longer periods for storage during excess generation.

An interesting difference between the two facilities is the significantly shorter maximum discharge time of the Huntorf CAES. At maximum power, it can discharge its stored energy within 2 hours, compared to 26 hours for the McIntosh plant. This may affect the ability of the Huntorf facility to meet peak demand.

Up until very recently, all commercial scale CAES projects have been diabatic. In 2019, a commercial A-CAES project was completed in Goderich, Ontario by the company Hydrostor[17]. However, compared to the two prior diabatic facilities, it has a relatively small nameplate power output capacity of 1.75 MW and a charging capacity of 2.2 MW. Its storage capacity is 10 MWh.

This year, two more CAES facilities have opened in China. The first was a 60 MW facility in Changzhou City, Jiangsu province in May 2022[18]. Its efficiency is over 60% and its energy storage capacity is about 300 MWh. The second Chinese CAES project was a 100 MW facility in Zhangjiakou, Hebei province which connected to the grid in September 2022[19,20]. It has a rather high efficiency of over 70% and an energy storage capacity of 400 MWh.

The facility in Zhangjiakou is unique and has been labeled “advanced” CAES by the Chinese Academy of Sciences. Various innovations have allowed the facility to run without using fossil fuels to heat turbine input air and to have an efficiency superior to any of the other currently existing commercial projects. Some of these innovations involve supercritical heat exchange and thermal storage as well as high load compression and expansion. Another distinct aspect of this project is its use of an artificial air storage vessel rather than a natural cavern.

Several other utility scale CAES projects are planned by Hydrostor. The largest of these is the Gem Energy Storage Facility, also known as the Willow Rock Energy Storage Center[21,22]. It is being built in Kern County, California. It is expected to have a nameplate power output capacity of 500 MW and an efficiency of around 60%. Its energy storage capacity is expected to be 4 GWh. Unlike the Huntorf and McIntosh facilities which only have one compressor and turbine train, the Gem facility will have five separate compressor and turbine trains. Each turbine train will have a generation capacity of 100 MW. This facility will be an A-CAES process, and hot water will be used for thermal energy storage. Hydrostor does not use salt caverns for air storage; rather, they dig their own caverns into the bedrock. Hydrostor expects commercial operation of this facility to start in 2026 or 2027.

Another of Hydrostor’s upcoming facilities is planned for San Luis Obispo, California, and is referred to as the Pecho project[23,24]. Like the rest of Hydrostor’s projects, it will use an A-CAES process. The expected nameplate power capacity is 400 MW and energy storage capacity is 3.2 GWh. This facility will also have multiple compressor and turbine trains. Each of the four turbine trains will have a generation capacity of 100 MW.

One more of Hydrostor’s projects is the Broken Hill A-CAES facility, planned for New South Wales, Australia. The nameplate capacity of this facility will be 200 MW and the energy storage capacity will be 1.6 GWh.

Analysis of CAES Compressor, Turbine, and Stored air

Fundamentally, the energy which is stored in CAES is the electrical energy input into the compressor which pressurizes air. The energy recovered is from depressurizing that stored gas through a turbine.

In this section, we will consider a simplified CAES system with one compressor and one turbine. A cooler unit is included after the compressor and a heater is included to reheat air before it enters the turbine. The process flow diagram of this system is shown in Figure 3.

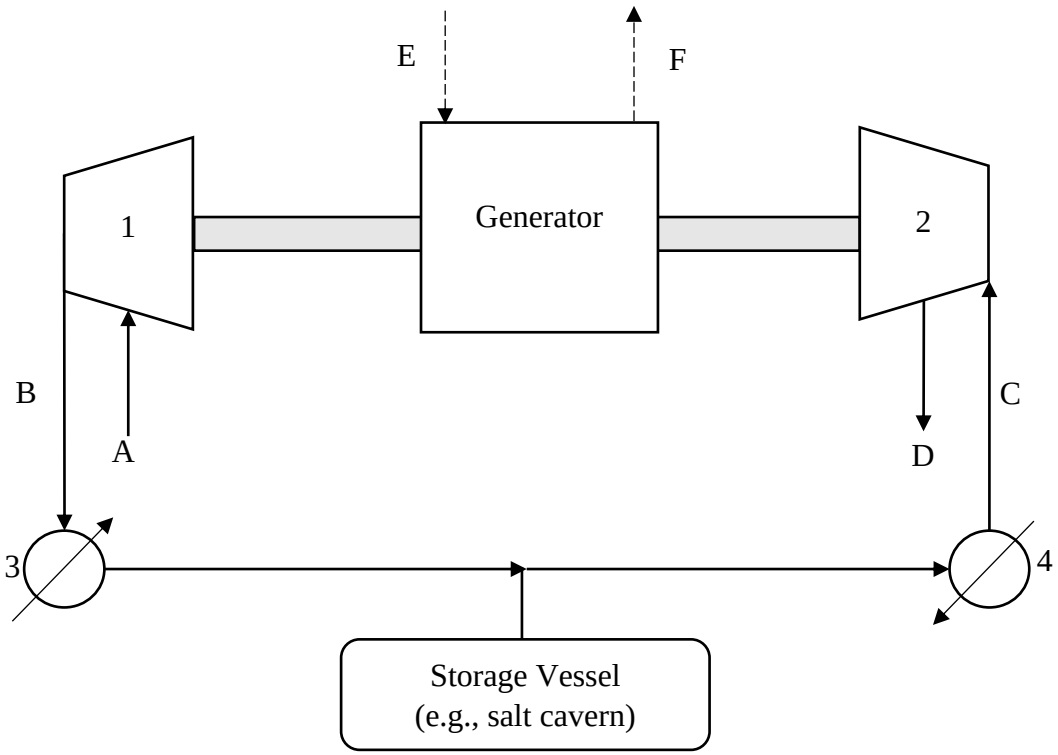

Figure 3. Simplified CAES process flow diagram. 1: Compressor. 2: Turbine. 3: Cooler. 4: Heater. A: Input Ambient Air. B: Compressor Outlet Air. C: Turbine Inlet Air. D: Output Air. E: Input Compressor Work. F: Output Turbine Work.

The work done on a gas during compression and during expansion in a turbine may be expressed as

[1a] $\delta W_{compressor} = V_m dP$;

[1b] $\delta W_{turbine} = -V_m dP$,

where V_m is the molar volume of the gas in and dP is the differential change in pressure. $\delta W_{compressor}$ is the differential molar compressor input work and $\delta W_{turbine}$ is the differential molar turbine output work.

The ideal gas law was used in this simple analysis. The equation of state of a gas may be represented by $PV_m = ZRT$, where the compressibility factor Z = 1.0 for an ideal gas. For air, the compressibility factor is generally between 0.96 and 1.04 conditions that may occur in a CAES process (T>270 K and P<100 bar)[25]. Therefore, the ideal gas law is sufficiently accurate for this purpose.

For an ideal gas, we may express the work done on the gas during isothermal compression by

[2] $W_{compressor,isothermal} = RT_{atm} \ln(\frac{P_{compressor,out}}{P_{atm}})$,

and for adiabatic compression by

[3a] $W_{compressor,adiabatic} = \frac{\gamma}{\gamma-1} K_{m,c}^{\frac{1}{\gamma}} \left(P_{compressor,out}^{\frac{\gamma-1}{\gamma}} - P_{atm}^{\frac{\gamma-1}{\gamma}} \right)$,

where $\gamma = \frac{C_p}{C_v} = 1.4$ is the specific heat ratio for air, $C_p = 29.07 \frac{J}{mol\ K}$ is the heat capacity of air at constant pressure, and $C_v = 20.76 \frac{J}{mol\ K}$ is the heat capacity of air at constant volume. These values are for air at ambient conditions. T_{atm} is the ambient air temperature, P_{atm} is the ambient air pressure, and $P_{compressor,out}$ is the pressure of the compressor outlet. $K_{m,c} = P_{atm} V_{m,atm}^{\gamma}$ is a constant for an adiabat. For ambient air, $K_{m,c} = (101{,}325\ Pa) \left(0.0224 \frac{m^3}{mol} \right)^{1.4} = 497 \frac{Pa * m^{4.2}}{mol^{1.4}}$. This gives

[3b] $W_{compressor,adiabatic} = 295 \left(P_{compressor,out}^{\frac{2}{7}} - P_{atm}^{\frac{2}{7}} \right)$,

where $W_{compressor,adiabatic}$ is in $\frac{J}{mol}$ and pressures are in Pa. The specific heat ratio γ of air does vary with temperature[26]; at 500°C it decreases to about 1.36. Therefore, for very large changes in pressure and temperature, this equation is not as good an approximation.

Using equations [2] and [3b], we can determine the work input of the gas compressor as a function of its outlet pressure. This dependence is shown in Figure 4.

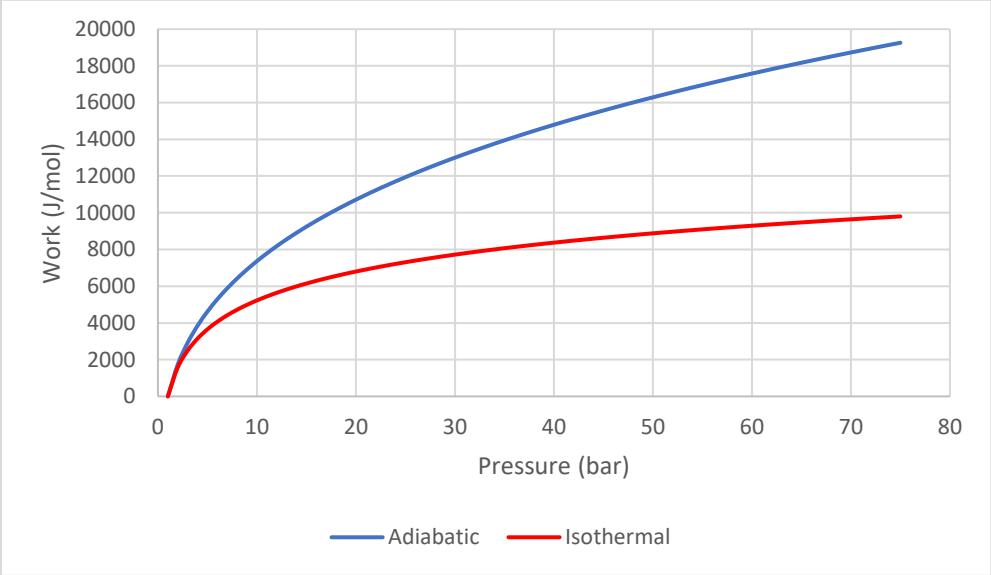

Figure 4. Work input to compressor to pressurize air to a given pressure $P_{compressor,out}$. The ideal gas equation of state is used to model air. The input air conditions are T = 273 K and P = 101,325 Pa.

Based on Figure 4, we can determine the work output of a compressor with an air flow rate of 100 kg/s which compresses air to 70 bar. This is about what the Huntorf and McIntosh facilities use. The isothermal work input is 33.3 MW and the adiabatic work input is 64.6 MW. This is compared to 62 MW and 53 MW for the compressor trains in the Huntorf and McIntosh facilities, respectively. This suggests that the compressors in existing CAES facilities may be more accurately modeled as adiabatic. This is not surprising since most compressors with a high compression ratio have good isentropic efficiency, meaning that the adiabatic assumption is valid[27].

Figure 4 shows that more work is required to pressurize air in an adiabatic compressor than an isothermal one for a given flow rate of air. In the adiabatic compressor, some of the work input goes into increasing the temperature of the gas rather than just its pressure. The difference between the curves for adiabatic work and isothermal work is reflective of the amount of work which goes into heating the air rather than pressurizing it. The temperature to which the adiabatic compressor heats air is given as a function of outlet pressure in Figure 5.

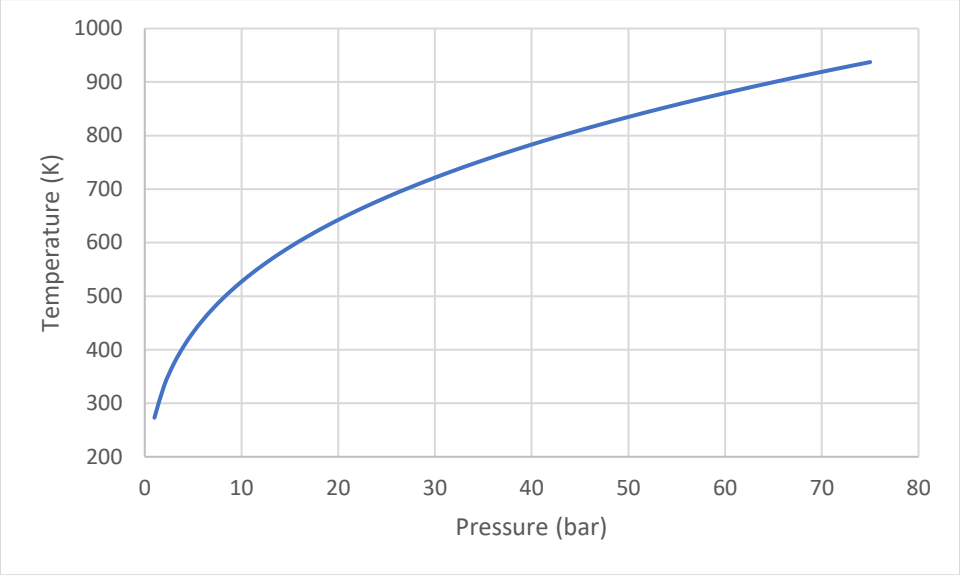

Figure 5. Outlet temperature of air from adiabatic compression. The ideal gas equation of state is used to model air. The input air conditions are T = 273 K and P = 101,325 Pa.

Even for low outlet pressures for CAES standards, the temperature of air increases significantly. For example, the pressures used for the Huntorf and McIntosh facilities yield a compressor outlet temperature over 900K. In reality, intercoolers are used between compressors in the train in order to prevent the air temperature from reaching such extremes (Figures 1 and 2).

For a turbine which expands air to atmospheric pressure, the work output may be expressed as

[4] $$W_{turbine,isothermal} = RT_{turbine,in} \ln(\frac{P_{turbine,in}}{P_{atm}}) ;$$

[5] $$W_{turbine,adiabatic} = \frac{\gamma}{\gamma-1} K_{m,t}^{\frac{1}{\gamma}} \left(P_{turbine,in}^{\frac{\gamma-1}{\gamma}} - P_{atm}^{\frac{\gamma-1}{\gamma}} \right),$$

where $T_{turbine,in}$ is the temperature of the air into the turbine and $P_{turbine,in}$ is the pressure of the air into the turbine. Note that the pressure of air into the turbine may not be the same as the pressure out of the compressor, $P_{compressor,out}$, due to heat losses with the environment or leakages. $K_{m,t} = P_{turbine,in} V_{m,turbine,in}^{\gamma}$ is a constant for an adiabat. $V_{m,turbine,in}$ is the molar volume of air into the turbine.

According to equations [4] and [5], the turbine output work in a CAES process depends both on the inlet temperature and pressure. Figure 6a displays the work output of the isothermal turbine for various inlet temperatures as a function of $P_{turbine,in}$, and Figure 6b displays the work output for the adiabatic turbine.

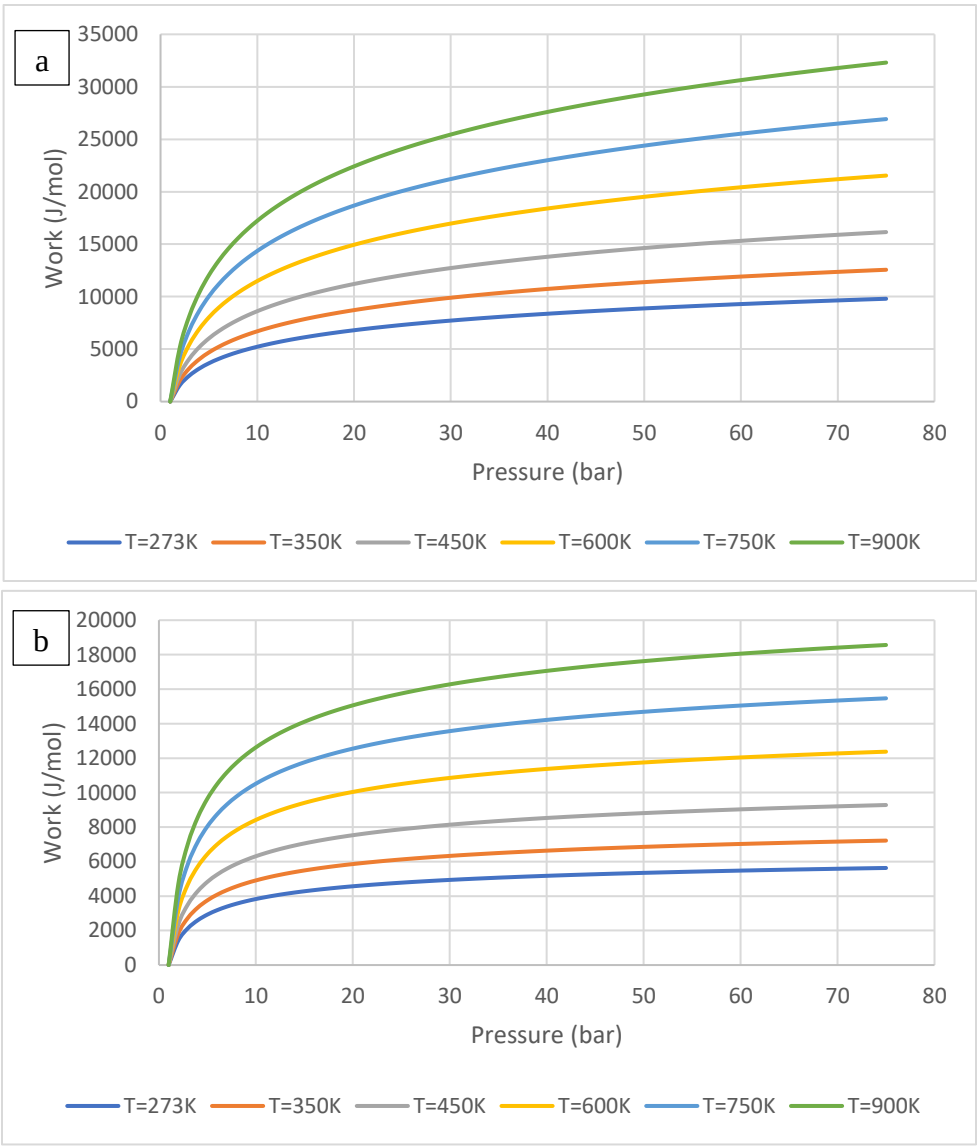

Figure 6. Work output from turbine to depressurize air to P_{atm} from a given pressure $P_{turbine,in}$. Ideal gas equation of state used to model air. Various $T_{turbine,in}$ displayed. **a** assumes isothermal expansion; **b** assumes adiabatic expansion.

Figure 6 indicates that for any given turbine inlet pressure and temperature, the isothermal turbine will always have greater work output than the adiabatic turbine. This is reflective of the theoretically high efficiency of isothermal CAES. It also highlights the importance of reheating the air prior to the turbine inlet in order to improve work output.

The total amount of energy which can be stored in compressed air is given as a function of the vessel volume and pressure

[6] $$E_{isothermal} = P_{vessel} V_{vessel} \ln\left(\frac{P_{vessel}}{P_{atm}}\right);$$

[7a] $$E_{adiabatic} = \frac{\gamma}{\gamma - 1} K^{\frac{1}{\gamma}} \left(P_{vessel}^{\frac{\gamma-1}{\gamma}} - P_{atm}^{\frac{\gamma-1}{\gamma}} \right) = 3.5 K^{\frac{1}{1.4}} \left(P_{vessel}^{\frac{2}{7}} - P_{atm}^{\frac{2}{7}} \right);$$

[7b] $$K = P_{vessel} V_{vessel}^{\gamma},$$

where P_{vessel} is the pressure of air stored in the vessel and V_{vessel} is the volume of the storage vessel. $E_{isothermal}$ is the energy storage capacity of the vessel if the expansion of stored air is performed isothermally, and $E_{adiabatic}$ is the energy storage capacity of the vessel if the expansion is performed adiabatically.

Equations [6] and [7] are used to determine the energy storage capacity of a CAES vessel per unit volume, shown in Figure 7.

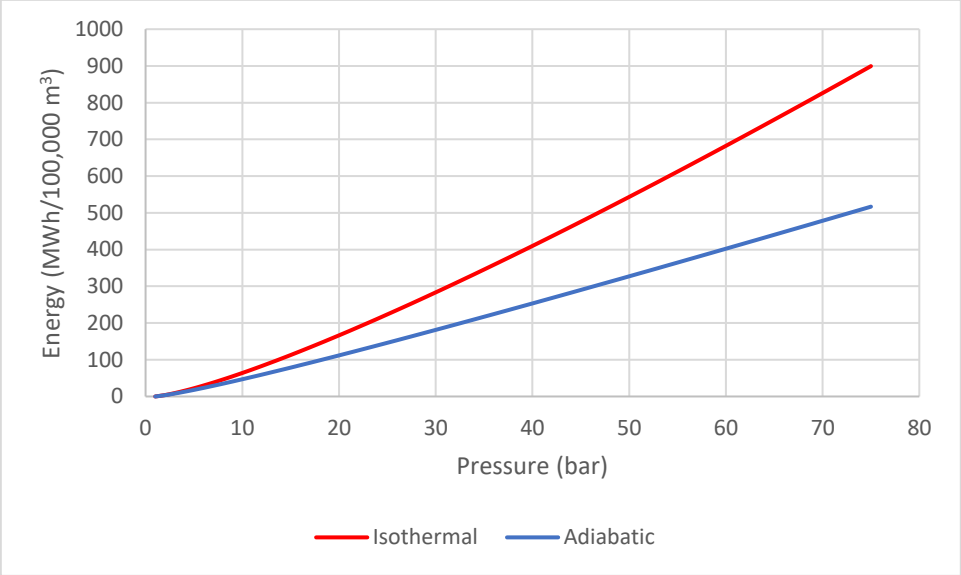

Figure 7. CAES energy storage capacity per 100,000 m^3 of storage vessel volume. Both isothermal and adiabatic turbines are considered. The ideal gas equation of state is used to model air. An ambient storage vessel temperature of 273K is assumed.

Figure 7 demonstrates that isothermal compression will store more energy than adiabatic for a vessel with a given pressure and volume. This can be explained by the nature of adiabatic expansion. The air will be cooled off during adiabatic expansion, such that the adiabatic work will always be less than the isothermal work (reflected in Figure 6).

For an adiabatic turbine condition with a storage vessel V = 560,000 m^3 and P = 74 bar, the energy storage capacity is predicted to be 2,851 MWh. This is similar to the maximum storage capacity of the McIntosh facility (Table 1), which has these same storage conditions.

For the adiabatic compressor condition with a vessel V = 310,000 m^3 and P = 70 bar, the energy storage capacity is predicted to be 1,483 MWh. This is significantly greater than the reported maximum energy storage capacity of 580 MWh for the Huntorf facility (Table 1), which has these same storage conditions. This suggests that the definition of maximum energy storage capacity is different between the Huntorf and McIntosh facilities. Another possible definition we will consider is the total energy which can be stored from a starting pressure of P = 43 bar, which is the minimum operating limit of the Huntorf facility. This gives a storage capacity of 630 MWh, which is in better alignment with the reported value and indicates that this is the definition Huntorf uses.

Applying this same definition of energy storage capacity to the McIntosh facility, we get a capacity of 1,055 MWh. Although the McIntosh facility can theoretically run for about 26 hours at the maximum power output, this result suggests that operating limits will keep this period to around 10 hours or less.

The efficiency of a CAES process can be represented as a ratio of compressor work input to turbine work output

[8a] $$\eta = \frac{W_{turbine}}{W_{compressor}},$$

where $W_{turbine}$ and $W_{compressor}$ are given in energy per mass or moles of air. If there is an external heating source, such as natural gas, the equation can be adjusted as such

[8b] $$\eta = \frac{W_{turbine}}{W_{compressor}+E_{external}},$$

where $E_{external}$ is given in energy per mass or moles of air. For example, the Huntorf facility uses 0.8 J of electricity and 1.6 J of natural gas to produce every 1 J of electricity[28]. This gives an efficiency:

$$\eta = \frac{1J}{0.8 + 1.6J} = 0.42$$

McIntosh facility uses 0.69 J of electricity and 1.17 J of natural gas to produce every 1 J of electricity[28]. This gives an efficiency:

$$\eta = \frac{1J}{0.69J + 1.17J} = 0.54$$

There are several sources of energy loss in a CAES process. First, there are small mechanical losses associated with the compressor and turbine. More importantly, the air which has been heated through adiabatic compression may lose heat to the environment. The greater the pressure the air is compressed to, the more heat is available to lose due to the elevated temperatures

(Figure 5). There may also be energy losses associated with the source of external heating, such as from a natural gas burner.

This inefficiency poses the question as to the usefulness of heating the gas with an external source. There is of course the practical consideration of preventing extremely low temperature turbine exhaust air, which could damage equipment. However, the extra energy input is also made up for as a benefit to the turbine work output. Figure 6 shows that higher temperature air input will produce much more turbine work than air at a temperature similar to that of the storage vessel. For example, an adiabatic turbine with input air at $T_{turbine,in} = 900\ K$ and $P_{turbine,in} = 70\ bar$ will produce a work output of 18,400 $\frac{J}{mol}$, versus 5,600 $\frac{J}{mol}$ for input air at $T_{turbine,in} = 273\ K$ (Figure 6b).

The enthalpy addition into the turbine inlet stream from external heating is given by

[9a] $$\Delta H_{air} = C_p(T_{turbine,in} - T_{vessel})$$

[9b] $$E_{external} = \frac{1}{\eta_{heater}} C_p(T_{turbine,in} - T_{vessel})$$

where ΔH_{air} is the molar or mass enthalpy change in the air between the cavern and turbine inlet, T_{vessel} is the temperature of the storage vessel, and η_{heater} is the efficiency of the heater. This equation assumes that the timescale for heat transfer is much shorter than the air storage period, such that it can be expected that the compressed air will come into thermal equilibrium with the storage vessel.

The enthalpy gain between vessel and turbine inlet would be about 18,200 $\frac{J}{mol}$ for the $T_{turbine,in} = 900\ K$ case. Assuming a natural gas heater with an efficiency of 60% is used, 30,400 $\frac{J}{mol}$ would need to be input into the CAES system in exchange for a 12,800 $\frac{J}{mol}$ increase in turbine work output versus the T = 273 K case. Therefore, 42% of energy from the natural gas is regained from the turbine work output. Although this may seem low, it is better than the overall CAES process efficiency without reheating. Figure 8 displays the overall process efficiency of a D-CAES process depending on how hot the turbine input air is heated.

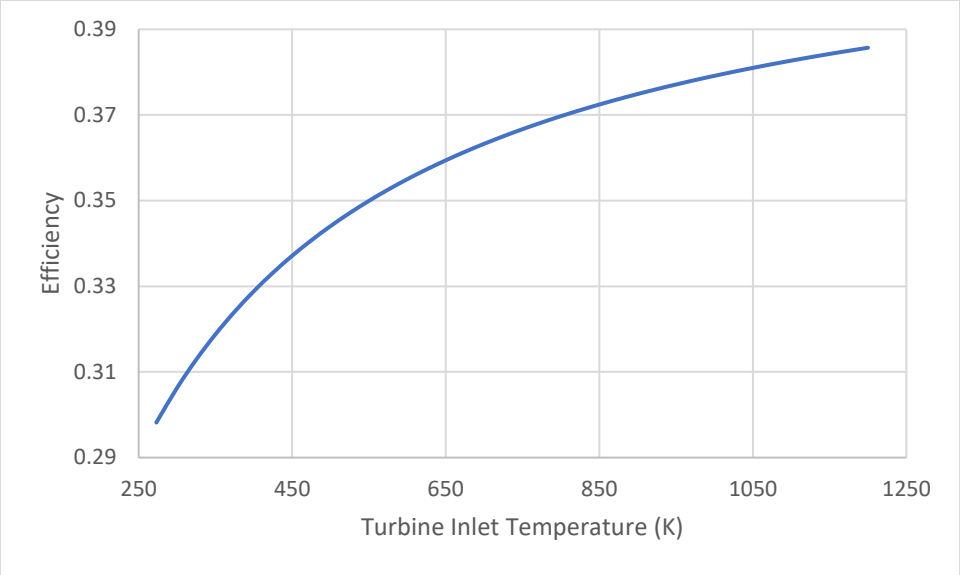

Figure 8. Efficiency versus reheating temperature for a simplified D-CAES process. Adiabatic compression and expansion are assumed. The ideal gas equation of state is used to model air. The input air conditions are T = 273 K and P = 101,325 Pa. An ambient storage vessel pressure of 70 bar and temperature of 273K is assumed. An efficiency of 60% is assumed for the natural gas heater. The losses in the compressor and turbine are assumed negligible. Cooling and heating are assumed to occur isobarically.

Figure 8 is not reflective of exact efficiency in a real D-CAES process but demonstrates that re-heating gas with a natural gas burner does in fact significantly improve the efficiency of the process, as opposed to running air at the ambient temperature of the cavern through the turbine. Although there are inefficiencies related to the natural gas burner, they are less significant than CAES with no reheating, which would only give about 30% efficiency. Therefore, using a natural gas burner actually increases overall CAES process efficiency. Ultimately, if the turbine inlet is heated hot enough, the overall process efficiency will approach that of the natural gas burner, assuming no inefficiency associated with the turbine.

Next, the efficiency of an A-CAES process will be examined. The air is reheated with only the heat which has been recovered from the compressed air. The turbine inlet reheating temperature versus efficiency for an A-CAES process is shown in Figure 9.

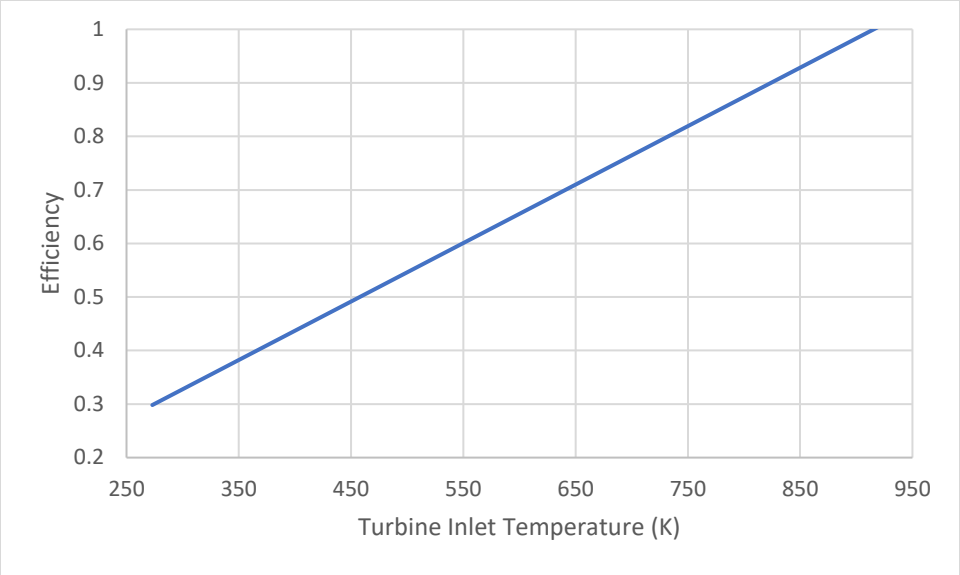

Figure 9. Efficiency versus reheating temperature for a simplified A-CAES process. Adiabatic compression and expansion are assumed. The ideal gas equation of state is used to model air. Input air conditions are T = 273 K and P = 101,325 Pa. An ambient storage vessel pressure of 70 bar and temperature of 273K is assumed. The losses in the compressor and turbine are assumed negligible. Cooling and heating are assumed to occur isobarically.

There is an upper limit to the turbine inlet temperature which can be achieved in A-CAES, which is equal to the outlet temperature from the compressor. In such a theoretical case where all the heat loss from the compressed air is recovered and used to re-heat the air later, the efficiency of a CAES process would be 100%. However, this would not occur in reality due to losses in the compressor and turbine. Furthermore, thermal energy storage systems used for A-CAES lose heat over time. Therefore, not all of the heat recovered can be put back into the air, such that the turbine inlet temperature will be less than the compressor outlet. This will limit efficiency. Ultimately, the actual efficiency of A-CAES will depend on the rate of heat loss in the thermal storage and the duration of storage.

A detailed discussion of the types of thermal energy storage used in A-CAES is beyond the scope of this project, but it will be noted that they can have respectable efficiencies. For example, an efficiency of 80% is reasonable for molten salt thermal energy storage[29]. Under the conditions represented in Figure 9, if this method of thermal energy storage was used, it would yield an overall process efficiency around 85%.

In summary, the performance of a CAES facility depends on several factors. They include the type of CAES, the compressor and turbine performance, the thermal energy storage system, and the storage conditions of the compressed air.

Process Simulation of CAES

We have used the Aspen Plus V11 software to simulate an A-CAES process. The purpose of this section is not a comprehensive process design, but rather an exercise to understand some important aspects of a real A-CAES process. Similar to existing CAES facilities, the process includes a compressor train consisting of a low- and high-pressure compressor, with coolers after each. The turbine train has a high- and low-pressure turbine with heaters before each. The CAES process is modeled as a pseudo-continuous process: an equal mass flow rate goes through the compressor and turbine at all times. While CAES does not actually work this way, simulating it like this is sufficient for analyzing process efficiency and stream properties.

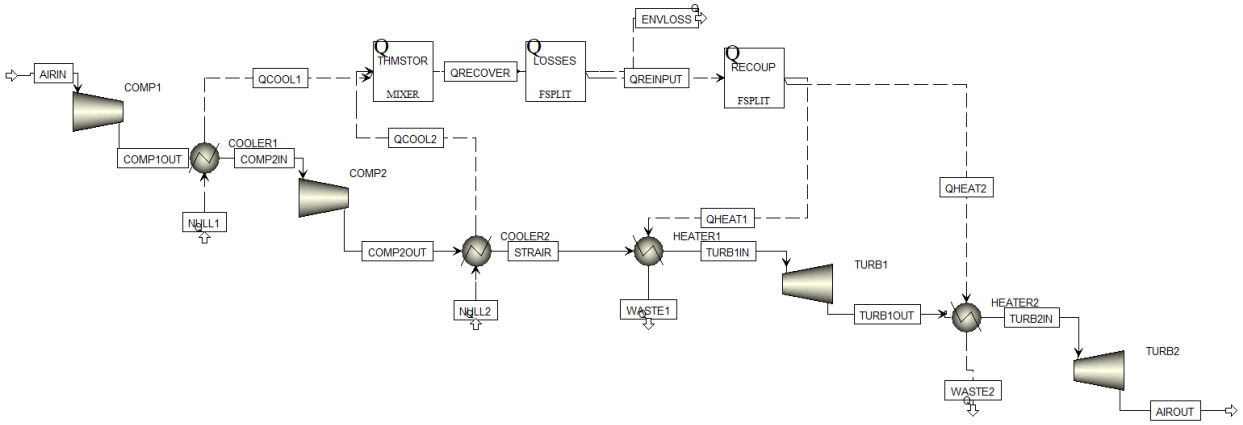

Figure 10. Process Flow Diagram of simplified A-CAES process in Aspen Plus V11.

For all Aspen CAES process simulations run, the Redlich Kwong Soave equation of state was used to model air. Air was assumed to have a composition of 79% nitrogen and 21% oxygen for the purposes of these simulations. The ambient input air was assumed to be at a pressure of 1 bar and a temperature of 290K. The air was modeled as being stored at 70 bar, the pressure of the Huntorf and McIntosh facilities, and with a temperature of 290 K, typical of salt caverns.

The first compressor pressurizes air to 35 bar and the second to 70 bar. The first turbine expands air to 35 bar and the second to 1 bar. The air flow rate through both the compressor and turbine trains is 400 kg/s. Of the recovered heat from the two coolers, 90% goes to the second heater and 10% to the first. This fraction was chosen to maintain above freezing temperatures in the turbine outlets and to keep in rough alignment with the work output of the respective turbines (Table A1).

The mechanical efficiency of the compressors and turbines were set at 95%, which is a typical value for most compressors and turbines. The isentropic efficiencies were set at 90% for the low-pressure compressor and turbine due to the high compression ratios (>3.5)[27]. These values were set to 60% for the high-pressure compressor and turbine due to the lower compression ratio (<3.5). The thermal energy storage and heat recover efficiency was set at 90%. These conditions represent “process 1” (see Tables A1 and A6 for process data).

We have initially assumed that heating and cooling of the air occurs isobarically, but in the original two CAES facilities the pressure generally decreases to about 50 bar (from 70 bar) after storage. This change was input into the simulation, and the first turbine was modified to expand the air to 25 bar. This process is referred to as "process 2" (see Tables A2 and A7).

Next, a design where all compressors and turbines have a high compression ratio was considered. The low-pressure compressor pressurizes air to 10 bar, and the high pressure turbine expands air to 10 bar. Therefore, an isentropic efficiency of 90% is assumed for all compressors and turbines. The recovered heat was split evenly between the first and second heaters to account for these changes, such that the input and output turbine temperatures were within an appropriate range and to reflect the similar power generation between the first and second turbines. This process is referred to as "process 3" (see Tables A3 and A8).

Current limitations in thermal energy storage technologies may limit its actual efficiency in an A-CAES process. A more realistic efficiency of heat recovery and thermal storage could be closer to 70%, especially over longer storage periods. This change is implemented in "process 4" to achieve more realistic conditions for an actual A-CAES process (see Tables A4 and A9).

A simulation with all the considered modifications of processes 2-4 was run. The output pressure of the low-pressure turbine was changed to 7 bar to maintain high compression ratios in both turbines. This simulation is referred to as "process 5" (see Tables A5 and A10). All five of the process simulations are summarized in Table 2.

Table 2. Performance of A-CAES process simulations in Aspen Plus V11. Equal input and outlet flow rate of 400 kg/s for each process.

Process	Input Work (MW)	Output Work (MW)	Overall CAES Efficiency (%)
1	287	207	72.3
2	287	195	68.0
3	230	174	75.8
4	287	176	61.4
5	230	142	61.6

These processes give overall CAES process efficiencies which are consistent with estimated efficiencies of recent and upcoming A-CAES facilities in the 60-70+% range. The process data also indicates which sources of inefficiency may be limiting or not. The mechanical and isentropic efficiencies of the compressors and turbines are typical of currently available equipment and are already rather high. Instead, these results suggest that thermal energy recovery and storage will present the greatest opportunity for improvement to A-CAES processes. Unlike gas compressor and turbine technology, which is mature and widely used in oil and gas applications, advanced thermal energy storage technology is still developing and is a topic of research.

It could be said that processes 1, 2, and 3 represent processes with advanced thermal energy storage technology (90% efficiency). The overall efficiencies of these processes are most similar

to that of the Zhangjiakou A-CAES facility, with 70+% efficiency, which is currently the most efficient CAES facility in operation. It is said to have cutting edge supercritical thermal energy storage, according to the Chinese Academy of Sciences[20]. Based on the results for processes 1, 2, and 3, it is very likely that the Zhangjiakou facility's thermal energy storage has an efficiency around 90% or perhaps even higher. This reflects the increasing maturity of A-CAES as commercial facilities start to come online or will within the next few years. We may expect to see more facilities with this level of performance soon.

Although current limitations in thermal energy storage could impact A-CAES efficiencies, an efficiency of around 60% is currently very achievable, as indicated by processes 4 and 5. The upcoming Gem Energy Storage Facility is also predicted to have a similar efficiency. This performance is still significantly better than the existing D-CAES facilities, while at the same time requiring no external heating.

Another result which is worth considering is that of process 2. A pressure drop in the air during storage from 70 to 50 bar (approximately 30%) was simulated. The impact on process efficiency is disproportionately small (4.3% decrease). In this process, the pressure drop was due to cooling of the air during storage, rather than leakage. This suggests that as long as the heat from the cooling air is recovered and reinput, output power will not be significantly decreased. On the other hand, significant leakage could reduce efficiency by virtue of reducing the total amount of air stored. Information on what fraction of stored air could leak out of a CAES storage vessel, namely a salt cavern, is not available and therefore was not considered in the design or results of the simulations.

The process improvement implemented in process 3 has been demonstrated to provide a modest improvement to the performance of the CAES process. Due to the higher isentropic efficiencies in the high-pressure compressor and turbine, it is expected that more of the input work will go toward changing the pressure of the air rather than changing its temperature. Therefore, more of the work can be recovered in the turbines.

We have highlighted several significant takeaways from these A-CAES process simulations. First, pressure losses during storage due to cooling have a relatively small effect on overall process efficiency. Moreover, the performance of the thermal energy storage system is the most limiting factor in overall A-CAES efficiency.

Finger Lake Salt Mines and CAES

There are three primary geological structures that are usable for CAES: hard rock, porous rock, and salt caverns[30].

Hard rock caverns are a less attractive option due to the high capital cost associated with creating new caverns (about $30/kWh). However, some planned commercial CAES facilities will be using such formations. This includes the Hydrostor A-CAES projects in California[21,22,23,24]. Although it is expensive, it allows for the locations of facilities to be less dependent on geology. Porous rock formations may offer a much less expensive form of storage, on the order of $0.10/kWh. Unfortunately, the storage period in the porous rock is limited. One study indicated that a reason for this was that air actually reacted with pyrite minerals in the porous rock[31].

Salt caverns are the most favorable of the three for CAES. Salt caverns have been used for petroleum gas and natural gas storage, and therefore extensive expertise on gas storage in these caverns is available. These salt caverns can be formed easily by solution mining, and the capital costs of this storage vessel are low, on the order of 2-10 $/kWh. This type of geological formation can be further divided into two types: salt domes and salt beds. The former is generally better for CAES applications due to being better suited for larger volumes and thus larger energy capacities.

Of the three types of geological structures, a potential CAES facility in the Finger Lake region would take advantage of salt caverns. For reference, the Huntorf and McIntosh plants took advantage of the salt dome geological formation. However, whereas the Huntorf and McIntosh plants had to form cavities in the salt domes via solution mining techniques, the proposed facility would take advantage of pre-existing caverns. Beneath the Finger Lakes region, there is a network of salt caverns due to salt mining in the area over the last century.

Around 550 million years ago, the New York region was at a sunken elevation. A cyclic process of evaporating salt water that left hundreds of feet thick salt layers and mudslides that covered up these layers created salt beds at varying depths beneath the surface[32]. In 1921, the Cayuga Rock Salt Company started the first underground salt mine and in 1970, this mine was acquired by Cargill Inc., who own the mines today. Of the many salt beds, there are only two that are of high enough quality and mineable: the No. 4 salt bed at a depth of approximately 2000 ft (600 m) and the No. 6 salt bed at a depth of approximately 2300 ft (700 m)[32].

The photograph in Figure 11 depicts an open area of the mine where several tunnels converge. In general, the mine workings are 42 ft wide and 10 ft high, according to American industrial[33].

Figure 11. Cargill Salt Mine[33]

A map of the Cargill mines is shown below in Figure 12. At a height of 10 ft and with over 3000 acres of tunnels underneath the lake, that amounts to over 37 million cubic meters of available volume for compressed air storage. Including the mined area beneath Lansing, that is an additional 20 million cubic meters. Assuming that all of the mine is useable space for compressed air storage and the air is stored at a pressure of 70 bar, this would equate to a theoretical energy storage capacity of approximately 272.7 GWh for a CAES application, assuming adiabatic expansion (equation [7] and Figure 7).

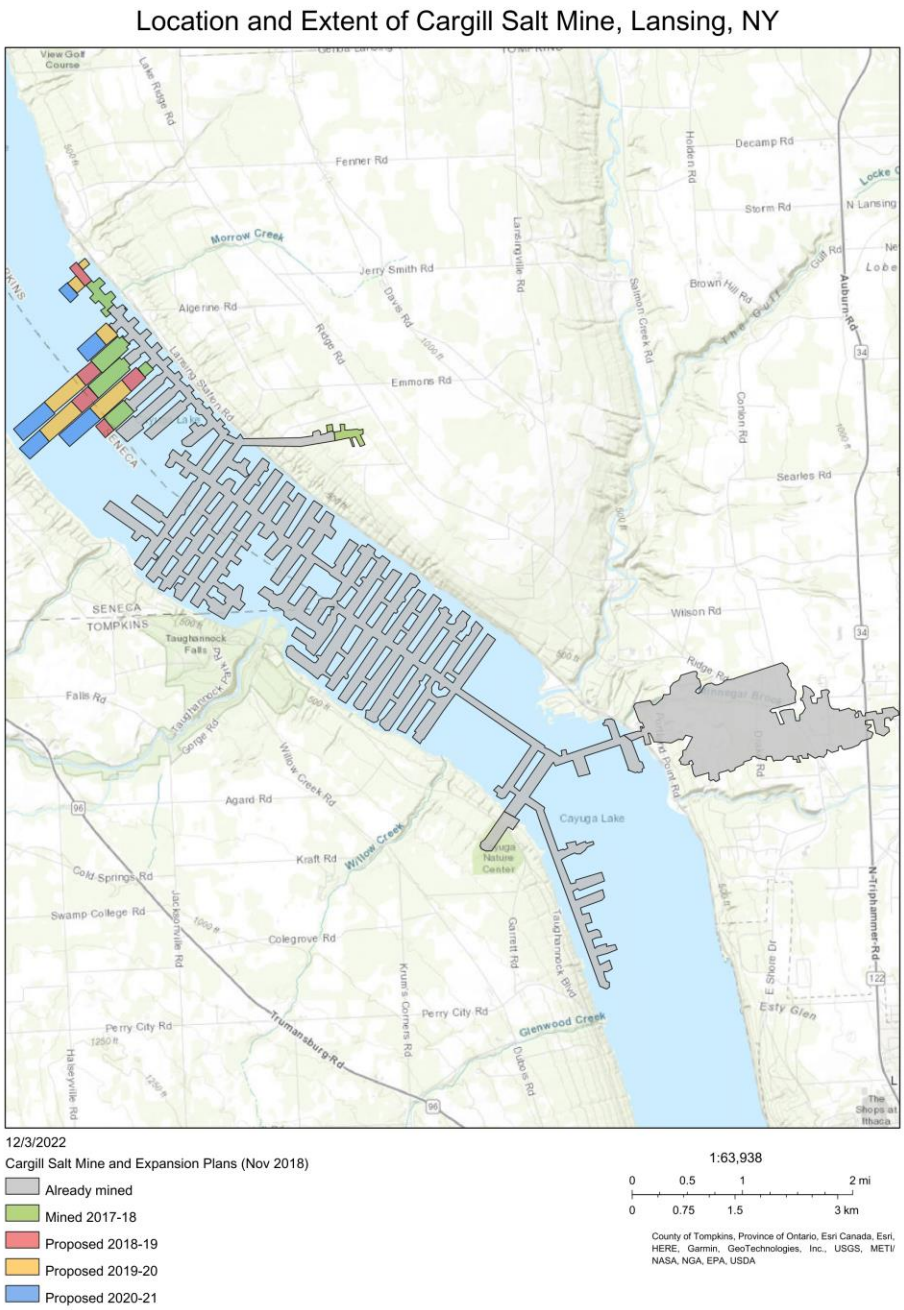

Figure 12. Map of the Cargill Salt Mine[34]. The map of the mine is taken from 2018 and since then, Cargill has primarily mined northwards along Cayuga Lake. The mines are primarily located beneath Cayuga Lake with some beneath the town of Lansing near Myers Point.

Any potential CAES facility on Cayuga lake would probably be situated on the east bank since some of the mines are directly beneath the land on that side. Most likely, the easternmost part of the mine, in Lansing and near the main entrance, would be used for CAES because this section alone represents a significant volume. Since Cargill is focusing on mining northwards, the portion of the mine south of the entrance could be considered as well.

The immense potential of Finger Lake salt mines for CAES was not overlooked as NYSEG considered it for the Seneca Lake salt mines in 2011 but considered it economically infeasible at the time[35]. However, the salt caverns were still found to have been suitable for CAES.

Three different CAES processes were considered by NYSEG for Seneca Lake[36], referred to as Cycle 1, 1A, and 2. They were all D-CAES processes that made use of natural gas combustion for air reheating. The storage vessel would be three salt caverns about 2,300 ft (700 m) below ground with a total free volume of 15,000,000 ft^3 (425,000 m^3). The processes were designed with the expectation that they would be cycled about 260 times per year. For all three processes, the compressor trains pressurize air to 1,500 psia (103 bar). The process flow diagrams for the three processes are displayed in Figure 13.

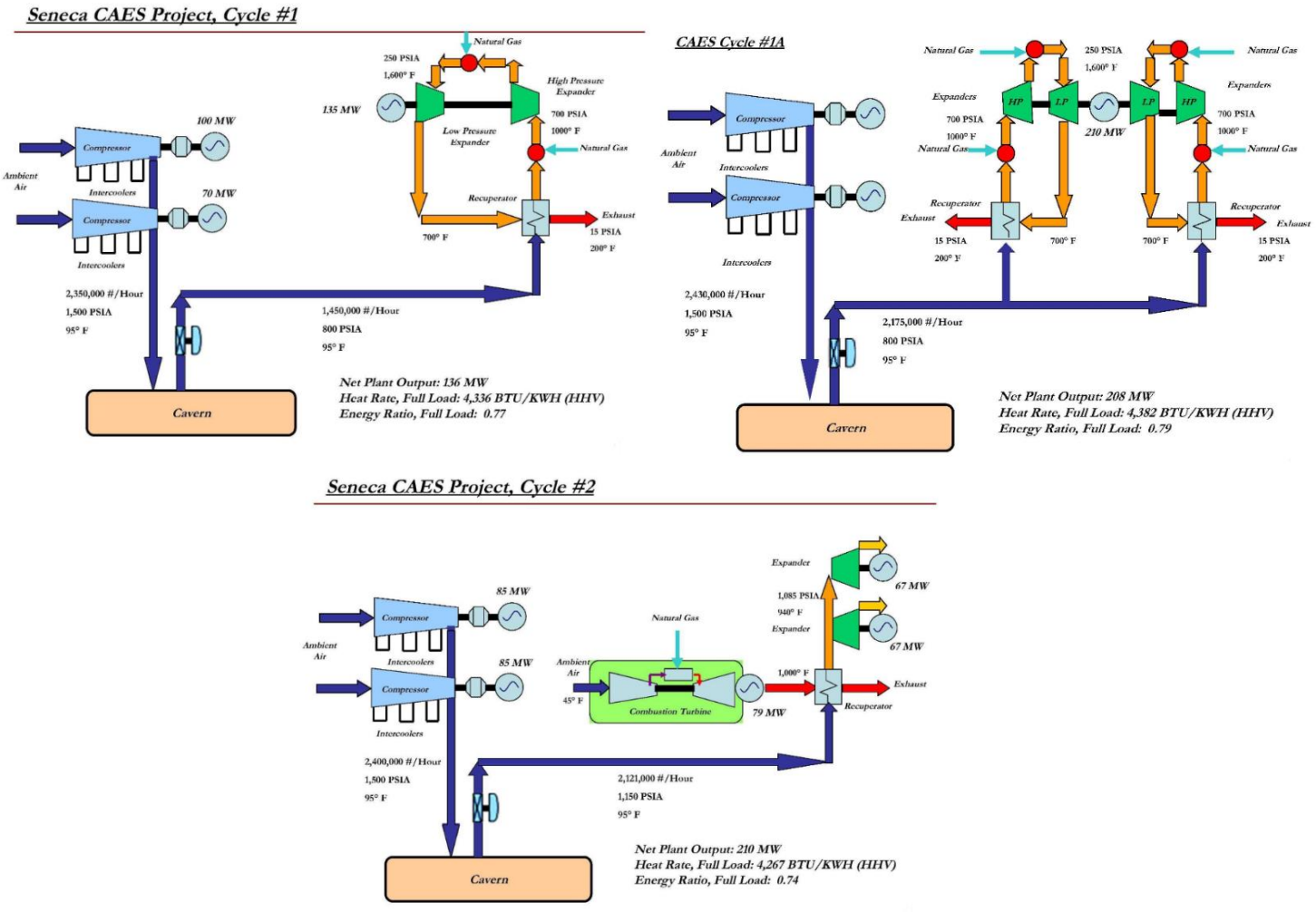

Figure 13. Process flow diagrams of the three proposed D-CAES processes for Seneca Lake by NYSEG[36].

Cycle 1 makes use of two parallel compressor trains with intercoolers. They are rated 100 MW and 70 MW, respectively. It has one turbine train with a 136 MW output. Cycle 1A has two parallel compressor trains, each rated 85 MW. It also has two parallel turbine trains, each with 105 MW rating. Cycle 2 has a similar compressor configuration to cycle 1A. There is a 79 MW natural gas combustion turbine, followed by two parallel air expansion turbines each rated to 67 MW. The process variables of the three proposed processes are summarized in Table 3.

Table 3. Proposed D-CAES processes for Seneca Lake. The energy storage capacity was estimated based on equation [7]. Efficiency was calculated based on equation [8b].

Process Variable	Cycle 1	Cycle 1A	Cycle 2
Nameplate Power Capacity (MW)	136	210	210
Compressor Rated Power (MW)	170	170	170
Energy Storage Capacity (MWh)	3,124	3,124	3,124
Compressor Air Flow Rate (kg/s)	274	293	280
Storage Pressure (bar)	55-103	55-103	79-103
Energy Ratio at Full Load	0.77	0.79	0.74
Heat Rate (BTU/kWh)	4,336	4,382	4,267
Overall Process Efficiency (%)	47.9	48.9	46.5
Time to turbine full load (min)	10	10	30
Time to compressor full load (min)	10	10	10
Capital Cost ($)	445.273M	497.178M	494.148M
Max Capital Cost for NPV=0 ($)	170.062M	225.737M	233.194M

Table 3 indicates that all three of the proposed CAES processes had excessive capital costs. NPV is a measure of all future and present cash flows, discounted to the present. If is not positive, then the project could be considered a poor investment. Out of the three, cycle 2 seems to be the closest to being profitable and it has the greatest NPV. However, it is also the least efficient and has a poor turbine start up time for peak loading applications.

The efficiencies of the three proposed processes are typical for D-CAES but still inferior to that of the Huntorf facility built over 30 years ago (Table 1). The storage pressures are also notably higher than that of the Huntorf or McIntosh facilities, and the pressure drop during storage was predicted to be much larger. Furthermore, Cycle 1 would be capable of generating electricity for about 23 hours, while Cycles 1A and 2 for about 15 hours. These discharge periods are within the range of existing CAES facilities. The average annual capacity factors, the ratio of average power output to nameplate capacity, for the three processes are shown in Figure 14.

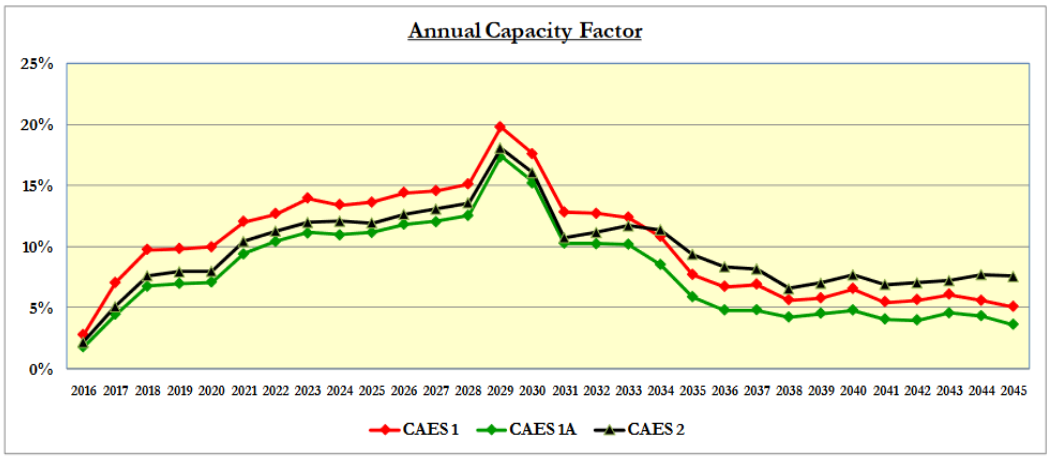

Figure 14. Projected annual capacity factors for proposed Seneca Lake CAES facility[36].

The capacity factors for all three of the proposed D-CAES processes would be less than 20%, which suggests that generation would typically be limited to less than five hours per day. An interesting feature of Figure 14 is that 2029 has an unusually high projected capacity factor. This could reflect changes to the mixture of energy generation technologies in NYS, for example more variable wind and solar renewable energy. More energy storage would be needed to support these variable generation sources. The ratio of discharge time and charging time was estimated for a future year is depicted in Figure 15.

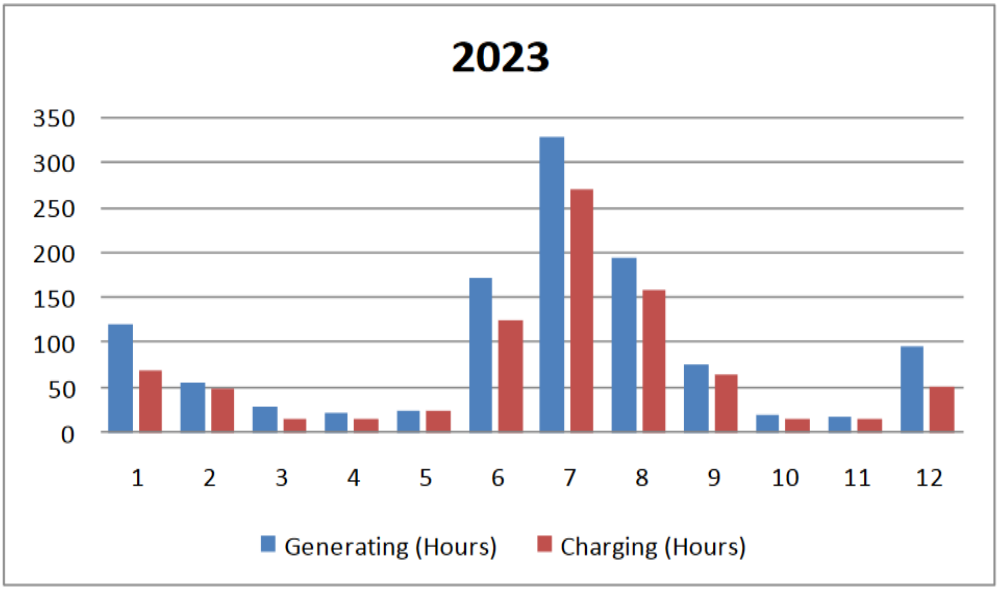

Figure 15. Generating and charging times for Cycle 1A CAES. Projected for 2023[36].

The chart indicates that the ratio of discharging to charging time is over one. This is particularly interesting because the existing Huntorf and McIntosh facilities have a ratio below one. Their compressor rated powers are much lower than their turbines, so these facilities would not be capable of the discharge pattern projected for the Seneca Lake CAES. This may reflect the

different energy loads and generation in NYS compared to Alabama or Germany, such that a higher ratio is desirable.

Since the proposed processes were D-CAES, there would be some associated emissions. However, compared to just combusting natural gas to generate electricity, there would be some emissions reductions which are summarized in Figure A1 in the Appendix. The emissions reductions could be as high as 150,000 Tons/yr. This is about 0.04% of the total 2019 NYS emissions, which was 379 MT CO_2 equivalents[37].

The project ultimately did not move ahead, but there will still be a significant need in NYS for energy storage. It is perhaps worth taking a second look at a Seneca Lake facility and performing a feasibility study for a Cayuga Lake CAES. Furthermore, the only type of CAES which was studied was D-CAES. Given the recent interest in A-CAES, it too should be investigated.

Regulatory, Community, Environmental and Safety Considerations

Although a CAES facility would have the potential to store a significant amount of energy, there are many safety concerns that must be addressed. Many of the concerns with implementing a CAES facility in the Cayuga salt mines are inherent to the caverns themselves. However, the storage of compressed air at high pressures and especially the cyclic charging and recharging of the facility would only serve to exacerbate any potential risks. As air is rapidly injected and withdrawn from the mine, the pressures and the temperature would change rapidly as well which is a cause for concern.

In general, the use of a salt cavern for CAES provides several benefits as compared to other geologies. Rock salt has a relatively very low permeability and thus can seal the compressed air with no leakage. Additionally, microfractures formed in the cavern may be closed as rock salt can self-heal. Rock salt also has a relatively high thermal conductivity, allowing for quick head dissipation when hot compressed air is injected[38]. Also, rock salt demonstrates elastoplastic properties. This means that even with many pressurizing and depressurizing cycles, the walls of the cavern can maintain their structural integrity over the long term[30]. Therefore, the risk of structural damage is low even for the decade's long lifespan of a CAES facility. Nonetheless, the caverns are not free of risk and the geology of the caverns must be closely studied to evaluate the safety risks.

One concern with using the caverns is the potential for the extreme pressures in the mines to increase the chances of a cavern collapse, forming a sinkhole on the surface. The depth at which a cavern must be located to avoid forming a sinkhole, the failure height, is dependent on the cavern geometry. Regardless of geometry, there is a linear correlation between failure height and the height of the cavern. For example, a 150 ft tall cavern with a cylinder chimney would have a failure height of 500 ft. In the case of the Cayuga salt mines, the cavern height is generally 10 ft but can be about 30 ft tall in some sections as seen in Figure 11. For a cavern height of 30 ft, the failure height would not surpass 500 ft[39]. Considering that the mines are 2300 ft below the

surface, the risk of a sinkhole forming due to cavern collapse is minimal. Of course, regardless of the impact to the surface, if the roof of the cavern collapsed, it would compromise the CAES facility.

A consideration unique to the Cayuga salt caverns is the presence of several anomalous points of thinner bedrock. These anomalies are above the mines and labeled as points A-E in Figure 16. The shaded red area represents the 1000 ft buffer that Cargill was supposed to avoid; however, the mines already extend underneath points C and E and infringes on the buffer zone of point D and B. As of 2018, there were plans to expand the mine further under anomaly point B. There is another anomaly, the Frontenac Point Anomaly (FPA), that has been infringed upon by the salt mines. In the 2016 map, the FPA was depicted as a yellow line on the map with 1000 ft buffer zone indicated by the shaded yellow region. Strangely, the FPA was redefined in 2018 to be the area represented by the blue oval.

These anomalies present not only an increased risk of cavern cave-ins, but subsidence as well. When a cavern exists beneath the surface, the bedrock above it will sag over time due to a phenomenon known as subsidence. This increases the likelihood that apertures for water seepage would be developed and alter the present pathways for groundwater and brine, further weakening the integrity of bedrock above the cavern[40].

The collapse of the mine presents not only a safety concern, but also an environmental one. If the cavern collapsed, a connection between the salt bed and the lake could be established, increasing the salinity of the lake. Such an increase would affect the wildlife in and around the Lake, as well as their habitat. Some of the community fear it may also affect the value of their property on the waterfront. Another environmental concern arises from the aforementioned change in water pathways. If groundwater pathways are significantly altered, this could affect the amount of groundwater available which would have a negative cascading effect. Decreased groundwater could lead to reduced local water levels and deteriorating water quality[40].

In 2013, Crestwood acquired the underground salt caverns beneath Seneca Lake. They planned to store millions barrels of liquid petroleum gas in depleted salt caverns. However, their plan was met with severe public backlash. Hundreds of regional businesses, half a million residents, and several senators across 17 municipalities all voiced their strong opposition to the plan. They cited leaks of brine and gas from the caverns, explosions and other catastrophic accidents, contaminated drinking water, impacts on tourism and the local wind industry, expansion of hydrofracking, and climate change as reasons for rejecting the storage plan. Ultimately, the project was rejected by former governor Cuomo in 2018[41,42,43].

Although many of the complaints about Crestwood's plan were centered around sustainability and anti-gas sentiment, it is not unlikely that similar complaints would arise regarding some of the safety issues. Therefore, despite benefiting from the attitude of sustainability, it is still necessary to ensure the safety of the facility to get the community's support.

In order to construct a CAES facility, a permit from the NY Department of Environmental Conservation (DEC) would have to be obtained. The land under Cayuga Lake is owned by New York State who permits Cargill to operate the mines. However, Cargill still owns the mines

themselves and as such, a contract or agreement would have to be determined with Cargill to use any areas of the mines that they are no longer mining. As Cargill primarily plans to mine further north along Cayuga Lake, a CAES facility could be proposed that uses the lower portion of the mine, south of Myer's Point. That portion of the mine still has roughly 22 million cubic meters of space for compressed air, which could store 105 GWh of energy.

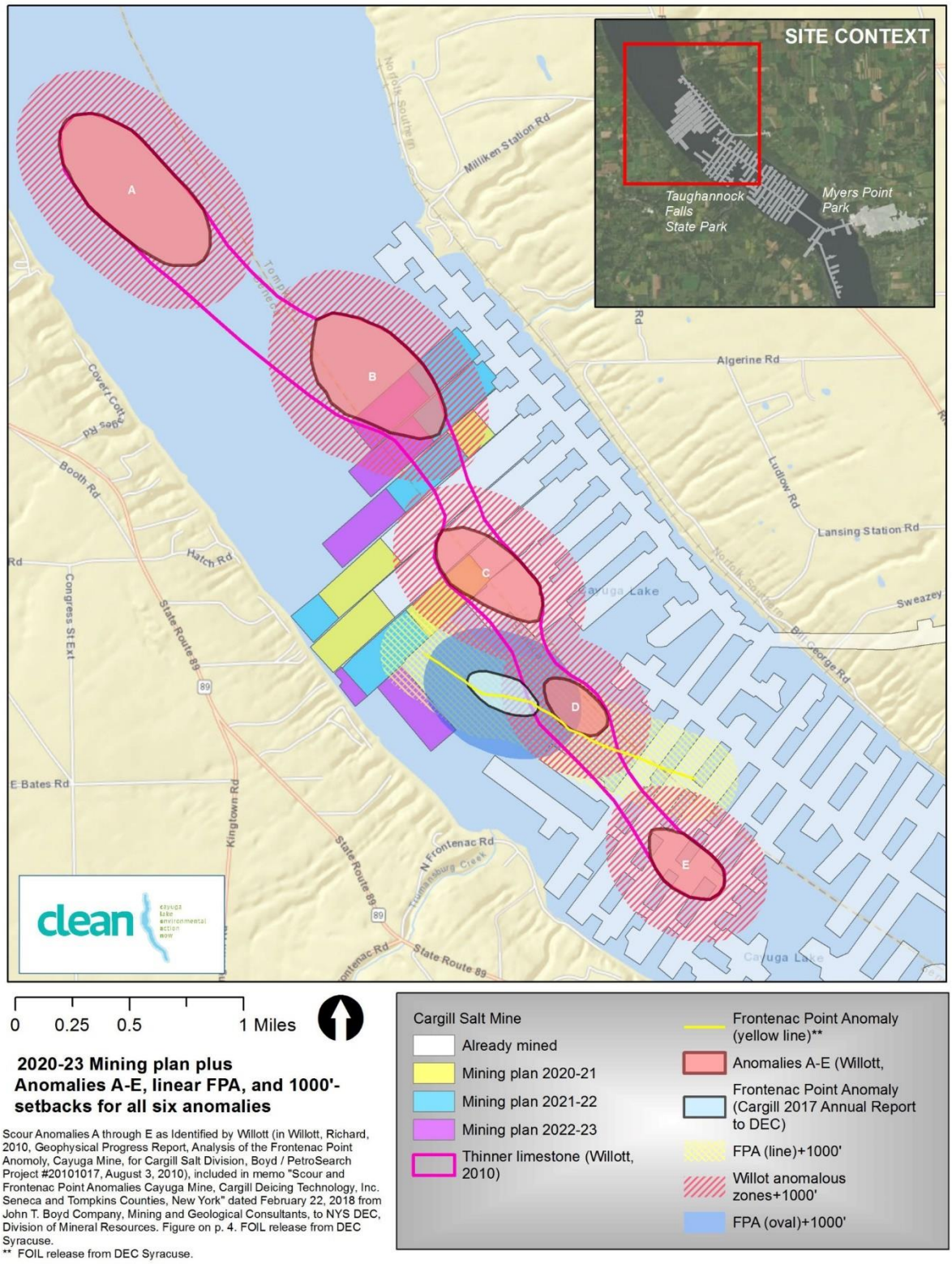

Figure 16. Anomalies above the Cayuga Salt Mines[39].

NYS Energy Needs

The NYS energy grid is operated mostly by the New York Independent System Operator (NYISO). They have published the 2022 Gold Book, which gives information on load and capacity data for NYS[44].

In NYS, the base load is about 12 GW. According to the NYISO, the typical coincident peak demand during summer 2021 in the New York Control Area (NYCA) was around 30.9 GW in summer. In winter 2021, the coincident peak demand was about 23.2 GW. By 2030, these figures are expected to increase to 31.7 GW and 27.7 GW, respectively. By 2050, these figures are expected to increase to 35.3 GW and 44.6 GW, respectively. The projected trends in summer and winter load are further summarized in Figure A2 of the Appendix.

As of 2022, variable renewable nameplate generating capacity in the NYCA is 1,818 MW for wind and 52 MW for large scale solar PV. Total wind energy production was about 4,100 GWh in 2021. This correlates to an average capacity factor of 25.7%. This is rather low, but typical for wind energy[45]. Planned projects would add another 10,158 MW of wind power and 7,109 MW of grid connected solar power. Under a scenario where total generating capacity does not increase significantly, this could mean that wind energy would account for a quarter of all electrical power generation in NYS. The variable nature of wind energy and its inherently low capacity factor mean that not all of these 10 GW of power will be available all the time. Even when wind power is being produced, it may be during times of low demand, such that not all of the generated power is actually used. However, energy storage provides a means to store the energy produced during times of low demand and then discharge it during periods of peak load. Therefore, NYS has a particularly strong need for energy storage.

NYISO reports on the state of energy storage in the NYCA. They predict that by 2030 the energy storage power capacity will increase to 4,314 MW for wholesale and 894 MW for behind the meter (BTM) storage. By 2050, these capacities are expected to be 10,607 MW and 1,734 MW, respectively. According to the NYISO, pumped hydro energy storage (PHS) already accounts for 4% of summer power generating capacity (1.409 GW) and 1% of yearly energy production (712 GWh). This indicates an average capacity factor of PHS in NYS of 5.8%. This value is low but similar to the projected capacity factor for the Seneca Lake D-CAES process (Figure 14).

Figure 17 gives an example load curve in NY for 2021 and projected for 2042. The load curves can demonstrate which times of day an energy storage facility such as CAES or PHS would be most likely to charge.

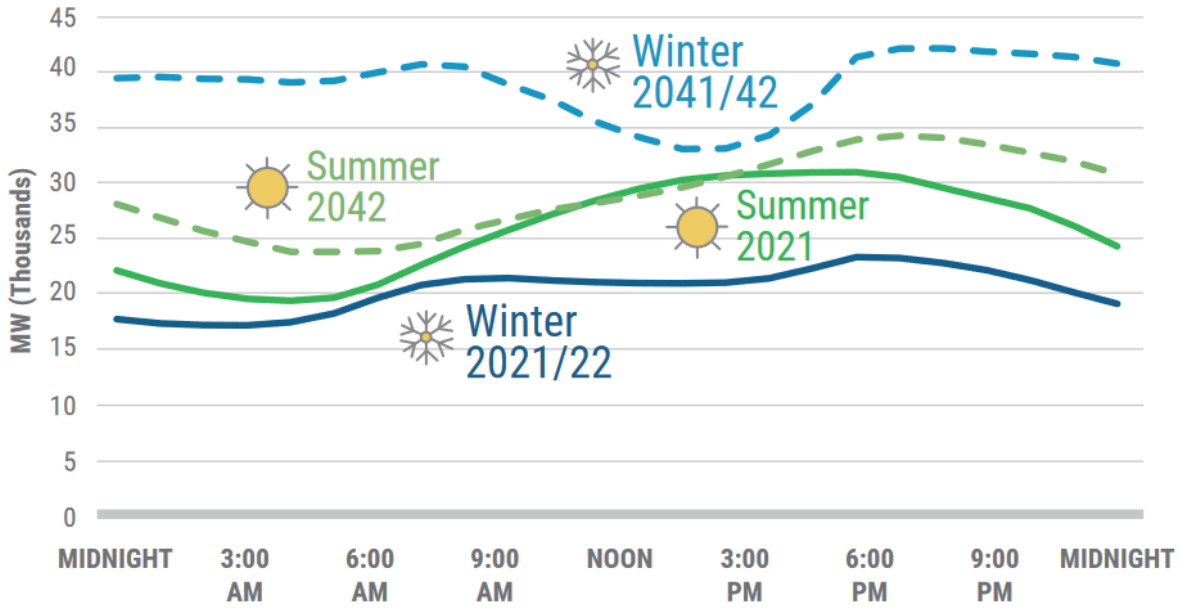

Figure 17. 2021 Actual and 2042 Forecasted Winter/Summer Load Curves[46].

During a typical summer day, the load is at a minimum around 12-9 am. Peak demand is usually around 3-7 pm. During the winter, the peak demand occurs around 5-7 pm, and minimum load occurs around 12-6 am. Therefore, a CAES facility in NYS would charge daily during the early morning hours, and then discharge for at least 2-4 hours in the late afternoon or early evening hours. The summer load curve is projected to maintain a similar shape by 2042, but the winter load curve is projected to significantly change. Peak demand will occur both around 7 am and 6 pm. There is also a considerable decrease in demand around 9 am to 4 pm, followed by a very sharp increase known as the Duck curve. During these winter months, a CAES facility would charge more often during the late morning and early afternoon hours. It would be required to quickly turn on its turbines around 5-6 pm in order to meet the peak load and manage the rapid increase in load.

For example, on July 27, 2022, one of the hottest days of the year, the hourly actual load across various regions of New York is shown in Figure A3. For this day, the CAES facility could be charged in the early morning, before 9 am. However, as it was a very hot day, the load remained high until around midnight. Conversely, on January 28, 2022, one of the coldest days of the year, the hourly actual load across various regions of New York is shown below in Figure A4. This figure indicates that in the winter, charging of the CAES facility could occur from 9 pm to 7 am when load is much lower. If variable sources such as solar and wind over-generated energy during the day, this energy could also be used to charge the CAES facility[47].

The current New York Control Area (NYCA) summer total generating capacity is 38.7 GW, and the winter generating capacity is 41.2 GW MW. In total, the annual energy production in 2021 was 126,766 GWh production 2021. This indicates an average generation of 14,471 MW over the entire course of 2021. The contributions from each fuel type are broken down below in Table 4.

Table 4. Summer and Winter Capacity in NYCA for 2021[44,46].

Generator Fuel Type	Summer 2021 Capacity (MW)	Winter 2021 Capacity (MW)
Gas	4,816.7	5,155.4
Oil	2,326.6	2,773.3
Gas & Oil	19,314.6	21,043.1
Nuclear	4,378.3	4,404.7
Pumped Storage	1,406.8	1,406.7
Hydro	4259.3	4,213.5
Wind	1,817.6	1,817.6
Solar	31.5	31.5
Other	319.0	326.2
Total	**38,670.4**	**41,172.0**

A CAES facility on Cayuga Lake could help to offset dependence on non-renewable energy sources for peak load applications in NYS. During peak hours, gas and oil are typically used to meet energy demands as they are fast and easily deployed. If the total generating capacity scales linearly with peak demand, then by 2030, the total necessary generating capacity would be 39,671.6 MW in the summer and 49,157.9 MW in the winter. By 2050, the total necessary capacity would be 44,176.9 MW in the summer and 71,149.6 MW in the winter. The CAES facility could be deployed to meet the increased capacity alongside the approximately 17 GW of wind and solar projects planned in the state.

There is an extensive network of electrical transmission and distribution lines throughout NYS, shown in Figure 18.

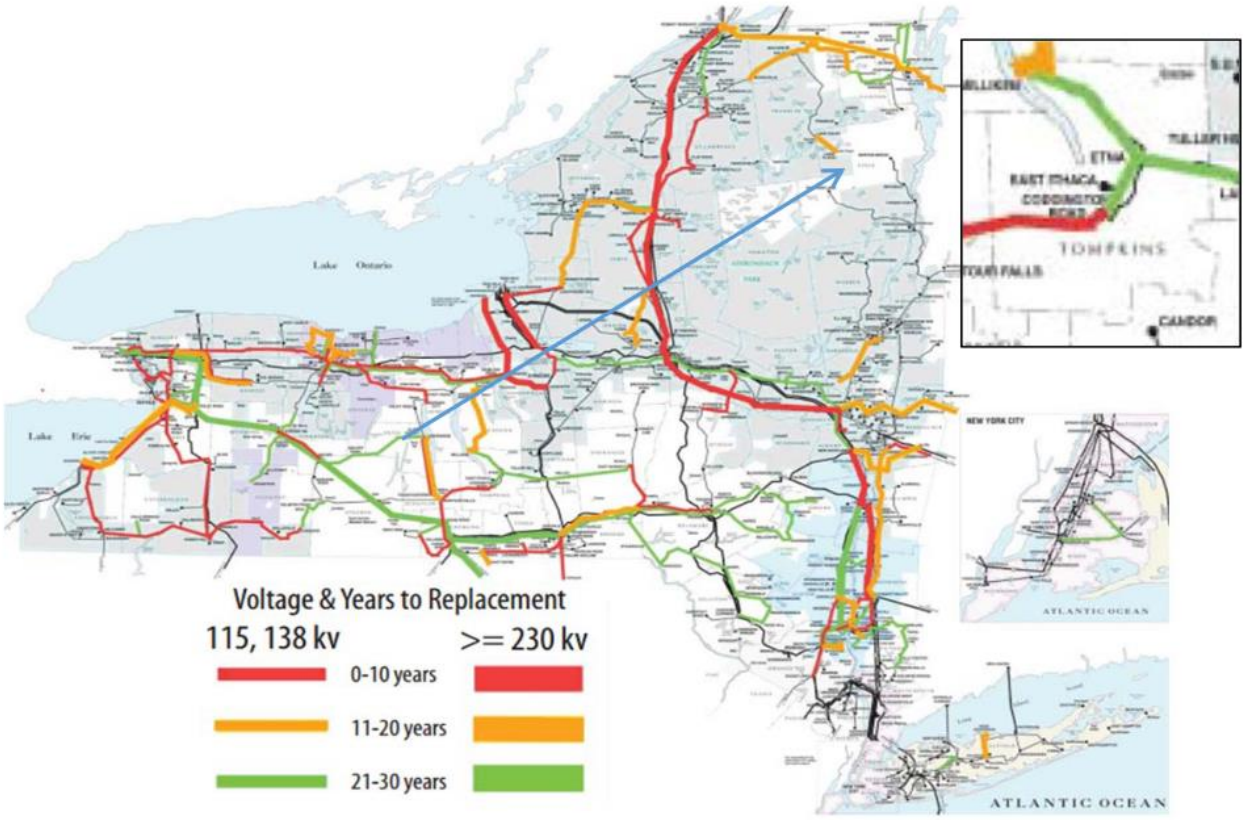

Figure 18. Transmission lines in NYS and around Cayuga Lake[48].

Although there are many transmission lines, few of them are particularly close to Cayuga Lake. There are three in total, and they are in the 115-138 kV range. One of these lines connects to the entrance of the Cayuga salt mines. If a CAES facility was constructed at the mines, it would be able to make use of this line. The years to replacement for this line is estimated at 11-20 years, which would be less than a typical lifetime for a CAES facility. Therefore, it would probably need to be replaced soon after the CAES facility is deployed. Regardless, other upgrades to the electrical transmission and distribution infrastructure would likely be necessary for a CAES facility to operate.

Essentially, there is a significant need for energy storage in NYS due to planned wind and solar projects, and the upwards trend of peak loads. Moreover, high-capacity storage technologies like CAES present a good alternative to fossil fuel peaking while preventing waste of variable renewable energy.

Recommendations and Comparison

Given the abundant salt mines in the Finger Lake regions, CAES is certainly a technically feasible choice for meeting NYS energy needs. We will compare it to other possible energy storage methods to determine if it is truly the best option and make recommendations based on this.

As seen in Figure 19 (and Figure A5), CAES presents one of the highest power output technologies available. A power output in the range of 10's to 100's of MW is possible, and CAES is capable of maintaining such an output for hours at a time[49,50]. Smaller scale energy storage technologies like batteries may be able to reach an output in the MW range but cannot maintain this power output for nearly as long as CAES can. This gives CAES a significant advantage in use for not only peak loading, but also for managing power demand over most of the day. Its energy storage capacity is also incredibly high compared to most other technologies, in the GWh range, and it is rivaled only by Pumped Hydro Storage (PHS) and hydrogen-based energy storage. Since grid scale hydrogen storage has not yet been implemented, the main technology that CAES should be assessed against is PHS.

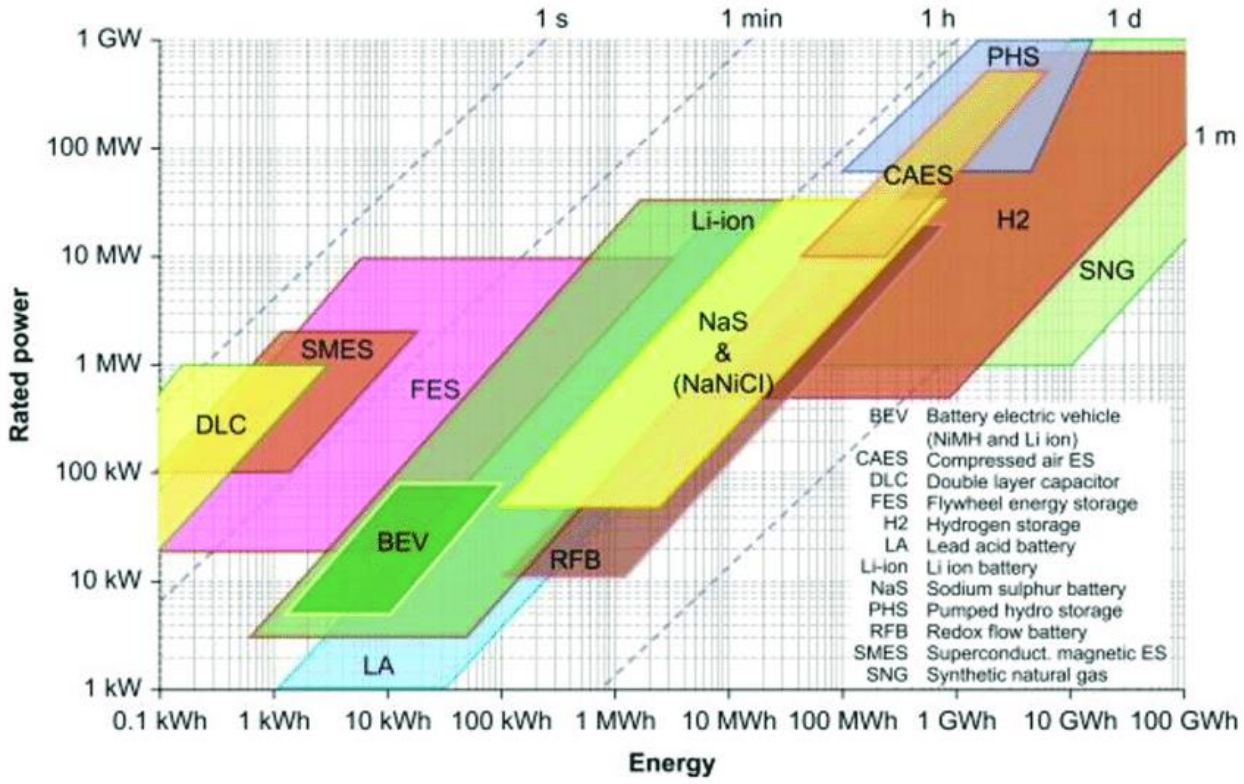

Figure 19. Comparison of energy storage technologies in storage capacity and rated power[50].

Some of the economic factors which must be considered in comparing these energy storage technologies are summarized in Table 5.

Table 5. Comparison of efficiency, lifetime, and capital costs of select energy storage technologies[51,52,53,54].

Storage Type	Efficiency (%)	Lifetime (years)	Power cost ($/kW)	Energy Cost ($/kWh)
CAES	40-70	35	400-800	1-50
PHS	70-90	30	2100-4300	5-80
Lead Acid Battery	70-80	4-8	1740–2580	300-500
Lithium Ion Battery	90	15	100-200	100-300
NaS Battery	60-80	15	1850-2150	300-500
Flywheel	90	20	3700-4300	1340-1570

PHS has a clear advantage over CAES in efficiency. Unlike CAES, PHS does not have significant heat losses to the environment. When the pressure of liquid water is increased by a pump, it does not get significantly hotter like air does through a compressor.

Both PHS and CAES can operate for long periods of time before decommissioning. In fact, the Huntorf facility has been in operation for 44 years and is said to still be very reliable even after so long[11]. Reportedly, its current availability is 90% and its starting reliability is 99%[55]. Batteries, however, can only go through many cycles before needing to be replaced, usually about a few thousand[56].

Notably, CAES has the lowest capital costs of any energy storage technology type according to many sources. The power-related costs are only slightly better than PHS, but its energy-related costs can potentially be much lower. The power-related costs of CAES are mostly associated with the equipment used (compressors, turbines, heaters). One of the main factors in the low costs of CAES is that this kind of equipment from oil and gas applications can be repurposed for CAES. Additionally, the energy-related costs are so low for CAES because they are mostly related to already existing underground storage caverns. Scaling up the energy storage capacity is as simple as using more cavern space. The significant economic advantages of CAES raise the question as to why so many PHS facilities exist but only a few CAES. In the US, there is 23.7 GW capacity for PHS but only 110 MW for CAES, according to Figure 20[57]. According to the NYISO, about 1.409 GW of this capacity is in NYS alone[43].

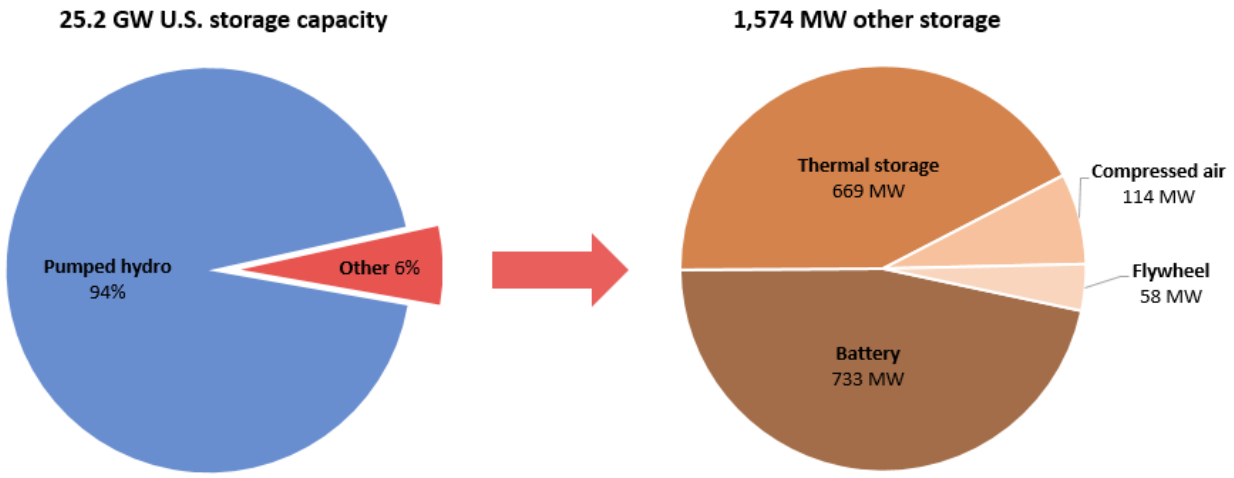

Figure 20. Energy Storage Capacity in the US by type[57].

The most important reason why CAES is not widely adopted is the need for specialized geology, specifically salt caverns, or other naturally existing underground vessels capable of storing compressed air. Without such natural features, the capital cost of CAES would be much higher, specifically in terms of energy-related costs, than indicated in Table 5. Therefore, CAES makes economic sense only in such places where caverns already exist, or when there is government support available for such projects. This may present an issue for the upcoming Hydrostor A-CAES projects, which will involve digging a cavern in hard rock. Fortunately, abundant salt mines are available in NYS Finger Lake region. CAES will prove much easier to implement here.

The capital cost of the upcoming Gem Energy Storage Facility is estimated to be about $1B[22]. Given that the power output will be 500 MW and the energy storage capacity will be 4 GWh, the power related costs and energy related capital costs are on the order of $1,000/kW and $100/kWh, respectively. This is higher than the estimated figures given in Table 5. Those estimates are based mostly on existing D-CAES facilities which use natural salt caverns. Since the Gem facility is an A-CAES process, which is a less mature technology, the costs are understandably higher. The thermal energy storage system is likely one of the contributors to increasing the power related costs. Furthermore, the energy-related costs are increased due to digging a cavern rather than making use of a natural one. For a potential Finger Lake A-CAES facility, we might expect the power-related capital costs to be similar to the Gem facility. However, due to the existing salt mines the energy-related costs would likely be quite low.

An additional cost which is not considered in the values in Table 5 is that of electrical transmission and distribution equipment. PHS systems are often situated alongside a hydroelectric facility, such as with the Robert Moses hydroelectric plant and Lewiston PHS plant at Niagara Falls[58]. Therefore, the PHS system may share its electrical transmission equipment, thus reducing costs. Therefore, for most CAES facilities, it might be expected that a significant amount of new equipment will have to be installed. However, on Cayuga Lake, there was until 2019 a 322.5 MW coal fired power plant[59]. It is only about a mile north of the most recent

sections of the salt mines. There is therefore likely still existing equipment which could be reused for a future CAES facility on the lake. Despite this, the existing transmission lines around Cayuga lake and the mines are not at a high voltage (<315 kV)[48,60], so if a very high output CAES facility is installed, upgrades will be needed.

We recommend that NYS considers installing an A-CAES process in the Cayuga lake salt mines. A-CAES is the best type of CAES to use for NYS energy needs due to the state's focus on reducing all electricity associated emissions by 2040[2]. We will present a process which could be installed on Cayuga Lake.

The proposed process is similar to that of the "process 5" simulation (Table 2), which has an efficiency of 61.6%, a storage pressure of 70 bar, and a storage temperature of 290 K. The turbine train containing a low- and high-pressure turbine will be scaled up to about 300 MW. Several compressor and turbine trains will operate in parallel. If we had five parallel trains like the upcoming Gem facility, this would give a total power generation capacity of 1.5 GW. If about 5,000,000 m^3 of the salt mines were used for the CAES facility (about 10% of the total mine volume), the energy storage capacity of the facility would be about 23.9 GWh according to Figure 7. We are assuming that the energy related to the depth of the caverns is negligible. For the Cayuga salt mines at a depth of 700 m, the difference in gravitational energy is only 200 $\frac{J}{mol}$, compared to 18,700 $\frac{J}{mol}$ needed to compress the air to 70 bar (Figure 4). With this capacity, the entire stored energy could be discharged within 16 hours. If we set a lower operating limit of 40 bar, the energy storage capacity would be 11.3 GWh and the time to discharge would be 7.5 hours. The ratio of turbine to compressor rated power for the proposed Cycle 1A and 2 Seneca Lake CAES (Table 3) is 1.24. With this same ratio, each of the five compressor trains for the proposed Cayuga facility would be rated at 240 MW. The features of the proposed A-CAES process are summarized in Table 6.

Table 6. Summary of our proposed A-CAES facility on Cayuga Lake.

Process Variable	Value
Nameplate Power Capacity	1.5 GW
Compressors Rated Power	1.2 GW
Total Energy Storage Capacity	23.9 GWh
Discharge Time	16 hours
Storage Volume	5,000,000 m^3
Operating Pressure	40-70 bar
Efficiency	61.6%

The proposed facility alone could meet half of the NYS energy storage power output goal for 2030. Although this goal could be met in full by using more turbine trains, it is probably a better choice to diversify energy storage types instead. Batteries have lower power output, energy storage capacity, and higher costs than CAES, but they are more scalable and can be installed closer to the source of electricity demand.

The use of multiple trains is a good choice in the proposed A-CAES process for several reasons. First, it better suits the extremely large energy storage capacity of the salt mines. Secondly, it makes the process scalable. While the Huntorf and McIntosh facilities are limited in scaling their output, for our proposed facility one would be able to select the number of turbine trains to use in order to easily scale the power output. This will be helpful to prevent overgeneration and better meet peak demand. Moreover, there is the practical consideration that gas turbines over 1 GW in capacity are not that common. However, those in the 300 MW range are readily available[61]. For example, the GT13E2-210 gas turbine from General Electric could be a good choice for this proposed facility.

To estimate the costs of the proposed A-CAES facility, the values from Table 5 in addition to estimates on the upcoming Gem facility were considered. If we assume similar power related costs to the Gem facility, this component of the capital cost will be about $1.5B. The energy-related costs will be much lower due to the existing mines. Using a low-end cost of $5/kWh, the energy related capital costs will be around $120M. Let us add an additional $150/kW to the capital cost to account for transmission and substation equipment which must be installed[62]. Although existing transmission equipment at Cayuga could reduce this cost, the high-power output of the proposed facility means that a significant expansion would be necessary. For this analysis, we will assume that the operating costs for a CAES facility are about $20/kW-yr[62]. We will also assume the total lifetime of the facility to be 45 years, similar to Huntorf.

The levelized cost of energy of the proposed A-CAES facility can be estimated by

$$[10] \quad LCOE = \frac{C_{capital} + \sum_{t=1}^{n} \frac{O_t}{(1+r)^t}}{\sum_{t=1}^{n} \frac{E_t}{(1+r)^t}},$$

where $LCOE$ is the levelized cost of energy, $C_{capital}$ is the capital cost, O_t is the total yearly operation costs, n is the lifetime of the facility, r is the discount rate, and E_t is the yearly electricity generation.

The LCOE of the proposed A-CAES facility was compared to that of a PHS system with equal power output and energy storage capacity. The power-related capital cost of PHS is taken to be $2,500/kW and the energy related as $10/kWh. This gives a power-related capital cost of $3.8B and an energy-related capital cost of $240M. We will include a $150/kW cost for electrical transmission and substation equipment[62]. The operating costs of a PHS facility are taken to be $18/kW-yr[62]. The lifetime of the PHS facility is taken to be 45 years. The average discharge duration for a single day is taken to be 4 hours. Four different discount rate combinations were used to calculate LCOEs. The results from these calculations are displayed in Table 7.

Table 7. Costs of proposed A-CAES facility and equivalent PHS facility.

Process Variable	A-CAES	PHS
Total Capital Cost	$1.85B	$4.25B
Operating Costs	$30M/yr	$27M/yr
LCOE, r=0.05	$61/MWh	$122/MWh
LCOE, r=0.075	$80/MWh	$164/MWh
LCOE, r=0.10	$99/MWh	$209/MWh
LCOE, r=0.125	$120/MWh	$256/MWh
LCOE, r=0.15	$141/MWh	$304/MWh

From the results in Table 7, we find that the LCOE for an A-CAES facility is likely lower than that for PHS, even considering when a higher discount rate for an A-CAES facility than a PHS facility. In reality, the discount rates for PHS are likely the same as or less than CAES due to the increased technological maturity of the former. These calculations do not represent a comprehensive economic analysis but provide a good general comparison between A-CAES and PHS for bulk power management and peak loading applications.

It should be noted that since A-CAES is a less mature technology than PHS, there could be more unexpected issues and risks associated with installing the proposed facility. Not only would this increase the discount rate, but it may also mean that the capital costs assumed for the analysis are underestimates. More information on the recent and upcoming A-CAES facilities is needed to make a better economic assessment.

The simple analysis conducted in this paper suggests that an A-CAES on Cayuga Lake is both economically viable and capable of significant power and energy storage capacity. Using even just a fraction of the available salt mines would allow for a facility capable of meeting a considerable amount of NYS energy storage needs.

Conclusions

Compressed Air Energy Storage (CAES) is a high-capacity electrical energy storage technology with relatively low capital costs. It is based on using energy to pressurize air and expanding air to recover energy. In this paper, we have considered the state of the technology and made recommendations for using CAES to meet NYS energy needs.

CAES facilities have been in operation for decades, namely the Huntorf and McIntosh facilities. These facilities make use of a D-CAES process, which uses an external energy source (natural gas) to reheat air prior to expansion. In recent years, there has been increasing interest in A-CAES, which reheats the air using heat recovered from the compressor outlet. A-CAES's advantages include relatively high efficiency (60-70%) and no process emissions.

We have conducted process simulations of an A-CAES process, which gave efficiencies ranging from 61.4-75.8%. The results from these simulations suggest that the thermal energy storage system is the most limiting factor to the overall process performance of A-CAES.

The Finger Lake salt mines present an ideal geology for CAES. The Cayuga Lake salt mines could potentially store up to 177 GWh of compressed air. A D-CAES facility was previously considered for Seneca Lake, would have been able to store about 3.1 GWh. Ultimately, its projected capital costs were too high, but it was found to be technically feasible.

Moving forward with the project necessitates a thorough investigation of the geology of the salt caverns and surrounding bedrock. While salt caverns tend to be relatively safe, a rigorous analysis must be completed both to convince the local community but also to ensure that the anomalous areas of thinner bedrock above the caverns pose little to no risk.

Variable renewable energy generation in NYS is expected to increase up to 17 GW, and energy storage needs will increase alongside it. Large scale energy storage facilities with good dispatchability like CAES will be needed to meet peak load in the future. CAES may also be helpful in displacing gas, oil, and coal peak loading.

We have conducted a comparison of various energy storage technologies to assess the viability of CAES. For large scale needs, the main alternative to CAES is PHS. Both have relatively low capital costs, long storage periods, and high storage capacities.

We proposed an A-CAES facility making use of the Cayuga salt mines. It would have a power capacity of 1.5 GW and an energy storage capacity of 23.9 GWh. The capital cost for this proposed facility and a similar PHS facility were estimated at $1.85B and $4.25B, respectively. Projected LCOE were similar or lower for the CAES facility. These results imply that if geology permits, CAES is competitive against PHS. We recommend further consideration of a CAES facility at Cayuga Lake.

References

1. *Annual energy outlook—U. S. Energy information administration(Eia)*. (n.d.). Retrieved November 21, 2022, from https://www.eia.gov/outlooks/aeo/index.php
2. *Our progress*. (n.d.). NYSERDA. Retrieved December 1, 2022, from https://climate.ny.gov/Our-Progress
3. Hadjipaschalis, I., Poullikkas, A., & Efthimiou, V. (2009). Overview of current and future energy storage technologies for electric power applications. *Renewable and Sustainable Energy Reviews*, *13*(6), 1513–1522. https://doi.org/10.1016/j.rser.2008.09.028
4. Lund, H., & Salgi, G. (2009). The role of compressed air energy storage (Caes) in future sustainable energy systems. *Energy Conversion and Management*, *50*(5), 1172–1179. https://doi.org/10.1016/j.enconman.2009.01.032
5. Luo, X., Wang, J., Dooner, M., Clarke, J., & Krupke, C. (2014). Overview of current development in compressed air energy storage technology. *Energy Procedia*, *62*, 603–611. https://doi.org/10.1016/j.egypro.2014.12.423
6. Budt, M., Wolf, D., Span, R., & Yan, J. (2016). A review on compressed air energy storage: Basic principles, past milestones and recent developments. *Applied Energy*, *170*, 250–268. https://doi.org/10.1016/j.apenergy.2016.02.108
7. He, W., & Wang, J. (2018). Optimal selection of air expansion machine in Compressed Air Energy Storage: A review. *Renewable and Sustainable Energy Reviews*, *87*, 77–95. https://doi.org/10.1016/j.rser.2018.01.013
8. Heidari, M., Mortazavi, M., & Rufer, A. (2017). Design, modeling and experimental validation of a novel finned reciprocating compressor for Isothermal Compressed Air Energy Storage applications. *Energy*, *140*, 1252–1266. https://doi.org/10.1016/j.energy.2017.09.03
9. *The paris compressed-air network- elevators and other modern conveniences*. (n.d.). Retrieved December 1, 2022, from http://www.douglas-self.com/MUSEUM/POWER/airnetwork/airnetwork.htm
10. Letcher, T. M. (Ed.). (2022). *Storing energy: With special reference to renewable energy sources (Second edition). Elsevier*.
11. *Huntorf more than 20 years—Club des argonautes | e-nautia*. (n.d.). Retrieved November 6, 2022, from https://e-nautia.com/clubargon/disk?p=8631946
12. King, M., Jain, A., Bhakar, R., Mathur, J., & Wang, J. (2021). Overview of current compressed air energy storage projects and analysis of the potential underground storage capacity in India and the UK. *Renewable and Sustainable Energy Reviews*, *139*, 110705. https://doi.org/10.1016/j.rser.2021.110705
13. S. Succar, R.H. Williams, "Compressed air energy storage: theory, resources, and applications for wind power", technical report, Energy Systems Analysis Group, Princeton Environmental Institute, Princeton University, 2008.
14. Foley, A., & Díaz Lobera, I. (2013). Impacts of compressed air energy storage plant on an electricity market with a large renewable energy portfolio. *Energy*, *57*, 85–94. https://doi.org/10.1016/j.energy.2013.04.031

15. Ter-Gazarian, A. (2011). Energy Storage for Power Systems. Second edition. United Kingdom: The Institution of Engineering and Technology.
16. Lemofouet-Gatsi, S. (2006). *Investigation and optimisation of hybrid electricity storage systems based on compressed air and supercapacitors*. EPFL.
17. Colthorpe, A. (2019, November 26). Grid-connected advanced compressed air energy storage plant comes online in Ontario. *Energy Storage News*. https://www.energy-storage.news/grid-connected-advanced-compressed-air-energy-storage-plant-comes-online-in-ontario/
18. Colthorpe, A. (2022, June 1). China's compressed air energy storage industry makes progress. *Energy Storage News*. https://www.energy-storage.news/chinas-compressed-air-energy-storage-industry-makes-progress/
19. *China turns on the world's largest compressed air energy storage plant*. (2022, October 5). New Atlas. https://newatlas.com/energy/china-100mw-compressed-air/
20. *World's first 100-mw advanced compressed air energy storage plant connected to grid for power generation—Chinese academy of sciences*. (n.d.). Retrieved December 1, 2022, from https://english.cas.cn/newsroom/research_news/phys/202209/t20220930_321008.shtml
21. Commission, C. E. (current-date). *Willow rock energy storage center*. California Energy Commission. https://www.energy.ca.gov/powerplant/caes/willow-rock-energy-storage-center
22. *Hydrostor CEO discusses proposed 500 MW compressed air energy storage facility in California*. (n.d.). New Project Media. Retrieved December 1, 2022, from https://newprojectmedia.com/news/hydrostor-ceo-discusses-proposed-500-mw-compressed-air-energy-storage-facility-in-california
23. Commission, C. E. (current-date). *Pecho energy storage center*. California Energy Commission. https://www.energy.ca.gov/powerplant/caes/pecho-energy-storage-center
24. *Pecho energy storage center – hydrostor*. (n.d.). Retrieved December 1, 2022, from https://www.hydrostor.ca/pecho-energy-storage-center/
25. *The ideal gas law*. (n.d.). Retrieved December 1, 2022, from https://www.engineeringtoolbox.com/ideal-gas-law-d_157.html
26. *Air—Specific heat ratio*. (n.d.). Retrieved December 1, 2022, from https://www.engineeringtoolbox.com/specific-heat-ratio-d_602.html
27. Simpson, D. A. (2017). Chapter eight—Gas compression. In D. A. Simpson (Ed.), *Practical Onshore Gas Field Engineering* (pp. 513–571). Gulf Professional Publishing. https://doi.org/10.1016/B978-0-12-813022-3.00008-0
28. *Compressed air energy storage*. (n.d.). Retrieved December 1, 2022, from http://www.eseslab.com/ESsensePages/CAES-page
29. Flueckiger, S. M., & Garimella, S. V. (2012). Second-law analysis of molten-salt thermal energy storage in thermoclines. *Solar Energy*, *86*(5), 1621–1631. https://doi.org/10.1016/j.solener.2012.02.028
30. Luo, X., & Wang, J. (2013). *OVERVIEW OF CURRENT DEVELOPMENT ON COMPRESSED AIR ENERGY STORAGE*.

https://www.cedren.no/Portals/Cedren/Overview%20of%20Current%20Development%20on%20Compressed%20Air%20Energy%20Storage_EERA%20report%202013.pdf
31. "Handbook of energy storage for transmission or distribution applications", EPRI 1007189, http://www.w2agz.com/Library/EPRI Sources & Reports/(2002) Handbook of Energy Storage for Transmission or Distribution Applications, EPRI 1007189.pdf.
32. July 09, ohtadmin | on & 2019. (2019, July 9). *History of salt fields of cayuga lake watershed—Tompkins weekly*. Tompkins Weekly -. https://www.tompkinsweekly.com/articles/history-of-salt-fields-of-cayuga-lake-watershed/
33. *Cayuga rock salt mine*. (n.d.). Retrieved December 5, 2022, from https://www.americanindustrialmining.com/cayuga-rock-salt-mine
34. *Map viewer*. (n.d.). Retrieved December 5, 2022, from https://www.arcgis.com/apps/mapviewer/index.html?webmap=c2e7ff4ab0424003b9fa5867459effad
35. *Nyseg seneca lake compressed air energy storage project*. (n.d.). RESPEC. Retrieved December 5, 2022, from https://www.respec.com/project/nyseg-seneca-lake-compressed-air-energy-storage-project/
36. None, N. (2012). *Seneca compressed air energy storage (Caes) project*. New York State Electric & Gas Corporation, NY (United States). https://doi.org/10.2172/1088675
37. *Statewide greenhouse gas emissions report—Nys dept. Of environmental conservation*. (n.d.). Retrieved December 5, 2022, from https://www.dec.ny.gov/energy/99223.html
38. Fazaeli, M. M. (2017). *Stability Assessment of Salt Cavern Roof Beam for Compressed Air Energy Storage in South-Western Ontario*. University of Waterloo. https://uwspace.uwaterloo.ca/bitstream/handle/10012/12586/Fazaeli_Mohammad_Mahdi.pdf?sequence=1&isAllowed=y
39. Voegeli, Sam. (2021). "Geomechanics of Cavern Storage" Retrieved December 5, 2022.
40. Mantius, P. (2021, July 19). As risks of a catastrophic mine flood under cayuga lake mount, cuomo's dec guards cargill's secrets. *Water Front- Peter Mantius*. https://waterfrontonline.blog/2021/07/19/as-risks-of-a-catastrophic-mine-flood-under-cayuga-lake-mount-cuomos-dec-guards-cargills-secrets/
41. *Businesses oppose gas storage in seneca lake salt caverns | new york sustainable business council*. (n.d.). Retrieved December 5, 2022, from https://nyssbc.org/businesses-oppose-gas-storage-in-seneca-lake-salt-caverns/
42. *Crestwood's Seneca Lake propane storage facility rejected by DEC*. (n.d.). Albany Bureau. Retrieved December 5, 2022, from https://www.pressconnects.com/story/news/2018/07/12/dec-rejects-plan-crestwood-propane-storage-facility-seneca-lake/779605002/
43. Site, O. (n.d.). *About crestwood*. We Are Seneca Lake. Retrieved December 5, 2022, from https://www.wearesenecalake.com/about-inergy/
44. *"Gold Book: 2022 Load and Capacity Data." New York Independent System Operator. April 2022. Retrieved September 8, 2022 from https://www.nyiso.com/documents/20142/2226333/2022-Gold-Book-Final-Public.pdf/cd2fb218-fd1e-8428-7f19-df3e0cf4df3e*

45. *Windexchange: U. S. Wind energy performance(Capacity factors) in 2017*. (n.d.). Retrieved December 5, 2022, from https://windexchange.energy.gov/maps-data/332
46. "*Power Trends 2022*." New York Independent System Operator. Retrieved September 8, 2022 from https://www.nyiso.com/documents/20142/2223020/2022-Power-Trends-Report.pdf/d1f9eca5-b278-c445-2f3f-edd959611903?t=1654689893527
47. *Error—Lcg consulting: Energyonline*. (n.d.). Retrieved December 5, 2022, from http://www.energyonline.com/Data/GenericData.aspx?DataId=13http://www.energyonline.com/Data/GenericData.aspx?DataId=13
48. *Tompkins County Energy Roadmap Evaluating Our Energy Resources*. (2016). Tompkins County Planning Department. https://tompkinscountyny.gov/files2/planning/energyclimate/documents/Energy%20Roadmap%203-25-16.pdf
49. Møller, K. T., Jensen, T. R., Akiba, E., & Li, H. (2017). Hydrogen—A sustainable energy carrier. *Progress in Natural Science: Materials International*, *27*(1), 34–40. https://doi.org/10.1016/j.pnsc.2016.12.014
50. Bignucolo, F., Caldon, R., Coppo, M., Pasut, F., & Pettinà, M. (2017). Integration of lithium-ion battery storage systems in hydroelectric plants for supplying primary control reserve. *Energies*, *10*(1), 98. https://doi.org/10.3390/en10010098
51. Inage, S.-I. (2009). *Prospects for Large-Scale Energy Storage in Decarbonised Power Grids*. International energy agency. https://iea.blob.core.windows.net/assets/6bb67be5-0b74-403f-ac02-395c3f3a0762/energy_storage.pdf
52. Rastler, D. (n.d.). *Overview of Electric Energy Storage Options for the Electric Enterprise*. Electric Power Research Institute. https://www.greentechmedia.com/images/wysiwyg/News/EPRIEnergyStorageOverview%20DanRastler.pdf
53. Schoenung, Susan & Hassenzahl, William. (2003). Long-vs. Short-Term Energy Storage Technologies Analysis A Life-Cycle Cost Study A Study for the DOE Energy Storage Systems Program. Sandia Report SAND.
54. *Worldwide—Lithium ion battery pack costs*. (n.d.). Statista. Retrieved December 5, 2022, from https://www.statista.com/statistics/883118/global-lithium-ion-battery-pack-costs/
55. S. Samir, "Large energy storage systems handbook", edited by Jonah G . Levine, CRC Press, pp. 112-152, 2011
56. Bocca, A., Sassone, A., Shin, D., Macii, A., Macii, E., & Poncino, M. (2015). An equation-based battery cycle life model for various battery chemistries. *2015 IFIP/IEEE International Conference on Very Large Scale Integration (VLSI-SoC)*, 57–62. https://doi.org/10.1109/VLSI-SoC.2015.7314392
57. US EPA, O. (2015, August 4). *Electricity storage* [Overviews and Factsheets]. https://www.epa.gov/energy/electricity-storage
58. *Niagara Power Project* . (n.d.). New York Power Authority (NYPA). https://www.nypa.gov/power/generation/niagara-power-project
59. Anbinder, M. H. (n.d.). End of an Era: Power plant shutting down after 64 years. *14850*. https://www.14850.com/082911026-milliken-power/

60. *State of New York ENERGY SECTOR RISK PROFILE*. (n.d.). US Department of Energy. https://www.energy.gov/sites/prod/files/2016/09/f33/NY_Energy%20Sector%20Risk%20Profile_0.pdf
61. *Ge gas power | general electric*. (n.d.). Gepower-V2. Retrieved December 5, 2022, from https://www.ge.com/gas-power
62. Mongird, K., Viswanathan, V., Alam, J., Vartanian, C., Sprenkle, V., & Baxter, R. (2020). *2020 Grid Energy Storage Technology Cost and Performance Assessment*. https://www.pnnl.gov/sites/default/files/media/file/Final%20-%20ESGC%20Cost%20Performance%20Report%2012-11-2020.pdf

Appendix

Table A1. Aspen V11 Simulation: Process 1 data for compressors and turbines.

Process Variable	Low-P Compressor	High-P Compressor	High-P Turbine	Low-P Turbine
Indicated horsepower (MW)	229.28427	43.0002952	-15.1432364	-202.9302
Brake horsepower (MW)	241.351863	45.2634686	-14.3860746	-192.78369
Net work required (MW)	241.351863	45.2634686	-14.3860746	-192.78369
Power loss (MW)	12.0675931	2.26317343	0.757161818	10.14651
Efficiency	0.9	0.6	0.6	0.9
Mechanical efficiency	0.95	0.95	0.95	0.95
Outlet pressure (bar)	35	70	35	1
Outlet temperature (°C)	558.461673	120.706176	33.0071722	81.8431579
Isentropic outlet temperature (°C)	503.806158	81.2786584	9.77896805	39.3303473

Table A2. Aspen V11 Simulation: Process 2 data for compressors and turbines.

Process Variable	Low-P Compressor	High-P Compressor	High-P Turbine	Low-P Turbine
Indicated horsepower (MW)	229.28427	43.0002952	-14.9808951	-190.284323
Brake horsepower (MW)	241.351863	45.2634686	-14.2318503	-180.770107
Net work required (MW)	241.351863	45.2634686	-14.2318503	-180.770107
Power loss (MW)	12.0675931	2.26317343	0.749044755	9.51421617
Efficiency	0.9	0.6	0.6	0.9
Mechanical efficiency	0.95	0.95	0.95	0.95
Outlet pressure (bar)	35	70	25	1
Outlet temperature (°C)	558.461673	120.706176	31.5209817	113.305736
Isentropic outlet temperature (°C)	503.806158	81.2786587	8.05317261	71.1946788

Table A3. Aspen V11 Simulation: Process 3 data for compressors and turbines.

Process Variable	Low-P Compressor	High-P Compressor	High-P Turbine	Low-P Turbine
Indicated horsepower (MW)	121.071643	97.4542702	-83.3844664	-100.206251
Brake horsepower (MW)	127.443835	102.583442	-79.2152431	-95.1959381
Net work required (MW)	127.443835	102.583442	-79.2152431	-95.1959381
Power loss (MW)	6.37219173	5.12917212	4.16922332	5.01031253
Efficiency	0.9	0.9	0.9	0.9
Mechanical efficiency	0.95	0.95	0.95	0.95
Outlet pressure (bar)	10	70	10	1
Outlet temperature (°C)	310.995459	252.977692	47.0666843	47.6085832
Isentropic outlet temperature (°C)	281.786699	230.999032	27.7305062	21.915478

Table A4. Aspen V11 Simulation: Process 4 data for compressors and turbines.

Process Variable	Low-P Compressor	High-P Compressor	High-P Turbine	Low-P Turbine
Indicated horsepower (MW)	229.28427	43.0002952	-14.5221288	-170.687305
Brake horsepower (MW)	241.351863	45.2634686	-13.7960223	-162.152939
Net work required (MW)	241.351863	45.2634686	-13.7960223	-162.152939
Power loss (MW)	12.0675931	2.26317343	0.726106439	8.53436523
Efficiency	0.9	0.6	0.6	0.9
Mechanical efficiency	0.95	0.95	0.95	0.95
Outlet pressure (bar)	35	70	35	1
Outlet temperature (°C)	558.461673	120.706176	21.5009951	25.5974938
Isentropic outlet temperature (°C)	503.806158	81.2786584	-0.68287871	-11.3639186

Table A5. Aspen V11 Simulation: Process 5 data for compressors and turbines.

Process Variable	Low-P Compressor	High-P Compressor	High-P Turbine	Low-P Turbine
Indicated horsepower (MW)	121.071643	97.4542702	-74.5475585	-74.5289947
Brake horsepower (MW)	127.443835	102.583442	-70.8201805	-70.802545
Net work required (MW)	127.443835	102.583442	-70.8201805	-70.802545
Power loss (MW)	6.37219173	5.12917212	3.72737792	3.72644974
Efficiency	0.9	0.9	0.9	0.9
Mechanical efficiency	0.95	0.95	0.95	0.95
Outlet pressure (bar)	10	70	7	1
Outlet temperature (°C)	310.995459	252.977692	13.2430838	21.9000894
Isentropic outlet temperature (°C)	281.786699	230.999032	-5.16039513	2.10303778

Table A6. Aspen V11 Simulation: Process 1 data for streams.

Process Variable	Air In	Compressor 1 Out	Compressor 2 In	Compressor 2 Out	Stored Air	Turbine 1 In	Turbine 1 Out	Turbine 2 In	Air Out
Temperature (°C)	16.85	558.4616730 49071	16.85	120.70617623 479	16.85	72.758482890 512	33.00717240641	558.49167066 7121	81.84310 6658
Pressure (bar)	1	35	35	70	70	70	35	35	1
Molar Enthalpy (kJ/mol)	-0.244 7818 4553	16.292 57377 37036	-0.4749 43003 92977	2.6264 959849 2804	-0.688 4953 3561	1.1189 304321 7815	0.0267 094770 982566	16.293 541369 0763	1.65 6997 6856 721
Mass Enthalpy (kJ/kg)	-8.484 5225	564.72 61512 81674	-16.462 26915	91.038 468785 0343	-23.86 4327	38.783 883092 5403	0.9257 923526 35497	564.75 968965 4336	57.4 3413 7706
Molar Entropy (kJ/mol-K)	0.003 5517 0475 7741	0.0057 32859 30375 469	-0.0267 52567 39665	-0.0234 412119 071844	-0.033 2261 9978	-0.0275 234967 333693	-0.0250 691439 495323	0.0057 340228 001087 9	0.00 9468 5067 8827
Mass Entropy (kJ/kg-K)	0.123 1076 5543 7791	0.1987 09891 72220 8	-0.9272 85929 93716	-0.8125 091569 6871	-1.151 6721 7818	-0.9540 075494 47855	-0.8689 358339 07075	0.1987 502203 30027	0.32 8193 2904 6436
Molar Density (kmol/cum)	0.041 4829 4618	0.4998 23244 52405	1.4583 78798 72658	2.0824 745415 3553	2.912 2150 7186	2.3902 270749 9408	1.3750 338298 3142	0.4998 053968 02655	0.03 3873 8138
Mass Density (kg/cum)	1.196 7994 7459	14.420 09913 43117	42.074 80761 13208	60.080 217682 1879	84.01 8561 5551	68.959 000511 7734	39.670 272154 0737	14.419 584220 4602	0.97 7272 9856
Enthalpy Flow (MW)	-3.393 8090	225.89 04605 1267	-6.5849 07661	36.415 387514 0137	-9.545 7311	15.513 553237 0161	0.3703 169410 54199	225.90 387586 1734	22.9 7365 5082
Average MW	28.85 0397	28.850 3972	28.850 3972	28.850 3972	28.85 0397	28.850 3972	28.850 3972	28.850 3972	28.8 5039
Mole Flows (kmol/sec)	13.86 4627 1393	13.864 62713 93449	13.864 62713 93449	13.864 627139 3449	13.86 4627 1393	13.864 627139 3449	13.864 627139 3449	13.864 627139 3449	13.8 6462 7139
Mass Flows (kg/sec)	400	400	400	400	400	400	400	400	400
Volume Flow (l/sec)	3342 24.74 5657	27739. 06034 03152	9506.8 76506 60522	6657.7 654913 9549	4760. 8527 5201	5800.5 481087 5206	10083. 117112 1402	27740. 050883 8828	4093 02.2 1736

Table A7. Aspen V11 Simulation: Process 2 data for streams.

Process Variable	Air In	Compressor 1 Out	Compressor 2 In	Compressor 2 Out	Stored Air	Turbine 1 In	Turbine 1 Out	Turbine 2 In	Air Out
Temperature (°C)	16.85	558.4616730 49071	16.85	120.70617632 6797	16.85	70.455659303 482	31.520981 6636	559.4777036 87013	113.3057359 26328
Pressure (bar)	1	35	35	70	70	50	25	25	1
Molar Enthalpy (kJ/mol)	-0.2447818 4553	16.29257377 37036	-0.4749 43003 92977	2.6264959877 9866	-0.6884 95335 61036	1.1189304321 7815	0.0384184 9765 1628	16.30525038 96297	2.5808 04610 62186
Mass Enthalpy (kJ/kg)	-8.4845225	564.7261512 81674	-16.462 26915	91.038468884 5345	-23.864 32778	38.783883092 5403	1.3316453 6298	565.1655426 64684	89.454 73411 44357
Molar Entropy (kJ/mol-K)	0.0035517 0475 7741	0.0057 32859 30375 469	-0.0267 52567 39665	-0.0234 412118 99896	-0.0332 26199 78483	-0.0246 854036 655166	-0.022 2346 9366	0.0085 75912 41177 133	0.0119 61840 93311 83
Mass Entropy (kJ/kg-K)	0.1231076 5543 7791	0.1987 09891 72220 8	-0.9272 85929 93716	-0.8125 091567 1608	-1.1516 72178 18514	-0.8556 347940 16515	-0.770 6893 4293	0.2972 54569 92222 4	0.4146 16161 09459 8
Molar Density (kmol/cum)	0.0414829 4618 9648	0.4998 23244 52405 5	1.4583 78798 72658	2.0824 745410 2761	2.9122 15071 86524	1.7306 396791 4866	0.987 7471 6537 9931	0.3578 72483 35200 7	0.0311 12950 84038 31
Mass Density (kg/cum)	1.1967994 7459	14.420 09913 43117	42.074 80761 13208	60.080 217667 5342	84.018 56155 51386	49.929 642153 5195	28.49 6898 0543	10.324 76329 16558	0.8976 20989 80912
Enthalpy Flow (MW)	-3.3938090	225.89 04605 1267	-6.5849 07661	36.415 387553 8138	-9.5457 31115	15.513 553237 0161	0.532 6581 4519	226.06 62170 65874	35.781 89364 57743
Average MW	28.850397	28.850 3972	28.850 3972	28.850 3972	28.850 3972	28.850 3972	28.850397	28.850 3972	28.850 3972
Mole Flows (kmol/sec)	13.864627 1393	13.864 62713 93449	13.864 62713 93449	13.864 627139 3449	13.864 62713 93449	13.864 627139 3449	13.864627 1393	13.864 62713 93449	13.864 62713 93449
Mass Flows (kg/sec)	400	400	400	400	400	400	400	400	400
Volume Flow (l/sec)	334224.745657	27739.06034 03152	9506.876506 60522	6657.7654930 1934	4760.852752 01353	8011.2731184 8368	1403 6.615 4672	38741.80828 17715	44562 2.3779 76096

Table A8. Aspen V11 Simulation: Process 3 data for streams.

Process Variable	Air In	Compressor 1 Out	Compressor 2 In	Compressor 2 Out	Stored Air	Turbine 1 In	Turbine 1 Out	Turbine 2 In	Air Out
Temperature (°C)	16.85	310.9954585754 97	16.85	252.9776920628 92	16.85	249.17769675 3237	47.066684278694	291.10961369 1365	47.60858 3164
Pressure (bar)	1	10	10	70	70	70	10	10	1
Molar Enthalpy (kJ/mol)	-0.2447818 4553	8.487630620 95489	-0.307687586 04499	6.721298423 98196	-0.688495335 61036	6.6038 050352 0055	0.5896 175956 75729	7.8819 179664 8667	0.65 4442 6358 1683
Mass Enthalpy (kJ/kg)	-8.4845225	294.1945846 40065	-10.66493413	232.9707413 51941	-23.86432778	228.89 823628 496	20.437 070297 1025	273.19 963437 0603	22.6 8400 7824
Molar Entropy (kJ/mol-K)	0.0035517 0475 7741	0.0051 12681 99762 162	-0.015794158 55300	-0.014475345 60693	-0.033226199 78483	-0.0146 994731 80285	-0.0128 507497 666094	0.0040 577123 069215 6	0.00 6498 7835 7571
Mass Entropy (kJ/kg-K)	0.1231076 5543 7791	0.1772 13573 94766 2	-0.547450298 29269	-0.501738173 88330	-1.151672178 18514	-0.5095 067869 73629	-0.4454 271349 37657	0.1406 466704 35496	0.22 5258 0278 4131
Molar Density (kmol/cum)	0.0414829 4618 9648	0.2049 95021 59009 5	0.415553414 94808 6	1.550738809 86379	2.912215071 86524	1.5620 154157 8384	0.3754 370602 85513	0.2122 145942 97463	0.03 7495 6583 2796
Mass Density (kg/cum)	1.1967994 7459	5.914187796 89682	11.98888107 90687	44.73943061 80256	84.01856155 51386	45.064 765177 8868	10.831 508312 8374	6.1224 753371 1867	1.08 1764 6360
Enthalpy Flow (MW)	-3.3938090	117.6778338 56026	-4.265973655	93.18829654 07764	-9.545731115	91.559 294513 984	8.1748 281188 41	109.27 985374 8241	9.07 3603 1296
Average MW	28.850397	28.850 3972	28.850 3972	28.850 3972	28.850 3972	28.850 3972	28.850 3972	28.850 3972	28.8 5039
Mole Flows (kmol/sec)	13.864627 1393	13.864 62713 93449	13.864 62713 93449	13.864 62713 93449	13.864 62713 93449	13.864 627139 3449	13.864 627139 3449	13.864 627139 3449	13.8 6462 7139
Mass Flows (kg/sec)	400	400	400	400	400	400	400	400	400
Volume Flow (l/sec)	334224.745657	67633.969994 9806	33364.247869 4994	8940.659156 23966	4760.852752 01353	8876.1 141530 6517	36929. 298159 3268	65333. 052070 4467	369766.2 0114

Table A9. Aspen V11 Simulation: Process 4 data for streams.

Process Variable	Air In	Compressor 1 Out	Compressor 2 In	Compressor 2 Out	Stored Air	Turbine 1 In	Turbine 1 Out	Turbine 2 In	Air Out
Temperature (°C)	16.85	558.4616730 49071	16.85	120.70617632 6797	16.85	60.148702914 924	21.50099513 1713	433.86043300 934	25.59749 3789
Pressure (bar)	1	35	35	70	70	70	35	35	1
Molar Enthalpy (kJ/mol)	-0.244 7818	16.29257377 37036	-0.4749 43003	2.6264959877 9866	-0.6884 95335	0.7172802300 1865	-0.3301 42729	12.321837379 4027	0.01 0846 0437
Mass Enthalpy (kJ/kg)	-8.484 5225	564.7261512 81674	-16.462 26915	91.038468884 5345	-23.864 32778	24.862057359 0803	-11.443 26461	427.09420234 2654	0.37 5940 8819
Molar Entropy (kJ/mol-K)	0.003 5517 0475 7741	0.0057 32859 30375 469	-0.0267 52567 39665	-0.0234 412118 99896	-0.0332 26199 78483	-0.0287 063599 979788	-0.0262 57216 20587	0.0005 618238 442696 68	0.00 4420 1468 0261
Mass Entropy (kJ/kg-K)	0.123 1076 5543 7791	0.1987 09891 72220 8	-0.9272 85929 93716	-0.8125 091567 1608	-1.1516 72178 18514	-0.9950 074447 49453	-0.9101 16281 02914	0.0194 736952 969808	0.15 3209 2182 9854
Molar Density (kmol/cum)	0.041 4829 4618 9648	0.4998 23244 52405 5	1.4583 78798 72658	2.0824 745410 2761	2.9122 15071 86524	2.4888 661830 8461	1.4332 70928 83288	0.5870 169212 17993	0.04 0264 9670 2141
Mass Density (kg/cum)	1.196 7994 7459	14.420 09913 43117	42.074 80761 13208	60.080 217667 5342	84.018 56155 51386	71.804 777959 6389	41.350 43559 20414	16.935 671340 2602	1.16 1660 2918
Enthalpy Flow (MW)	-3.393 8090 1883	225.89 04605 1267	-6.5849 07661 9268	36.415 387553 8138	-9.5457 31115 41588	9.9448 229436 3212	-4.5773 05845 5784	170.83 768093 7062	0.15 0376 3527 6123
Average MW	28.85 0397	28.850 3972	28.850 3972	28.850 3972	28.850 3972	28.850 3972	28.850 3972	28.850 3972	28.8 5039
Mole Flows (kmol/sec)	13.86 4627 1393	13.864 62713 93449	13.864 62713 93449	13.864 627139 3449	13.864 62713 93449	13.864 627139 3449	13.864 62713 93449	13.864 627139 3449	13.8 6462 7139
Mass Flows (kg/sec)	400	400	400	400	400	400	400	400	400
Volume Flow (l/sec)	3342 24.74 5657	27739. 06034 03152	9506.8 76506 60522	6657.7 654930 1934	4760.8 52752 01353	5570.6 599388 8092	9673.4 16840 06314	23618. 786168 1694	3443 34.7 4469

Table A10. Aspen V11 Simulation: Process 5 data for streams.

Process Variable	Air In	Compressor 1 Out	Compressor 2 In	Compressor 2 Out	Stored Air	Turbine 1 In	Turbine 1 Out	Turbine 2 In	Air Out
Temperature (°C)	16.85	310.9954585754 97	16.85	252.9776920602 39	16.85	196.2 2827 6518	13.24 3083 7618	204.6 8878 7060	21.9 0008 9432
Pressure (bar)	1	10	10	70	70	50	7	7	1
Molar Enthalpy (kJ/mol)	-0.244 7818 4553	8.48763 0620954 89	-0.30768 7586044 995	6.72129 8423899 91	-0.6884 95335 61036	4.983 2938 6852 942	-0.393 5228 1104	5.278 2663 9309 337	-0.09 7211 3594
Mass Enthalpy (kJ/kg)	-8.484 5225	294.194 5846400 65	-10.6649 3413979	232.970 7413490 97	-23.864 32778	172.7 2877 8532	-13.64 0117	182.9 5298 8705	-3.36 9498
Molar Entropy (kJ/mol-K)	0.003 5517 0475 7741	0.00511 2681997 62162	-0.01579 4158553 0028	-0.01447 5345607 0919	-0.0332 26199 78483	-0.015 0977 2362	-0.013 1319 1769	0.002 0270 0026 6805	0.00 4056 1884 7160
Mass Entropy (kJ/kg-K)	0.123 1076 5543 7791	0.17721 3573947 662	-0.54745 0298292 699	-0.50173 8173888 708	-1.1516 72178 18514	-0.523 3107 7162	-0.455 1728 5611	0.070 2590 0727 6516	0.14 0593 8519 1433
Molar Density (kmol/cum)	0.041 4829 4618 9648	0.20499 5021590 095	0.41555 3414948 086	1.55073 8809871 61	2.9122 15071 86524	1.253 6525 0455 723	0.294 4691 2403 5553	0.175 6676 6982 6704	0.04 0770 9189 4550
Mass Density (kg/cum)	1.196 7994 7459	5.91418 7796896 82	11.9888 8107906 87	44.7394 3061825 11	84.018 56155 51386	36.16 8372 7072	8.495 5511 9156	5.068 0820 4969	1.17 6257 2057
Enthalpy Flow (MW)	-3.393 8090	117.677 8338560 26	-4.26597 3655918	93.1882 9653963 88	-9.5457 31115	69.09 1511 4129	-5.456 0470	73.18 1195 4823	-1.34 7799
Average MW	28.85 0397	28.8503 972	28.8503 972	28.8503 972	28.850 3972	28.85 0397	28.85 0397	28.85 0397	28.8 5039
Mole Flows (kmol/sec)	13.86 4627 1393	13.8646 2713934 49	13.8646 2713934 49	13.8646 2713934 49	13.864 62713 93449	13.86 4627 1393	13.86 4627 1393	13.86 4627 1393	13.8 6462 7139
Mass Flows (kg/sec)	400	400	400	400	400	400	400	400	400
Volume Flow (l/sec)	3342 24.74 5657	67633.9 6999498 06	33364.2 4786949 94	8940.65 9156194 61	4760.8 52752 01353	1105 9.386 1448	4708 3.466 5086	7892 5.320 4816	3400 61.6 7871

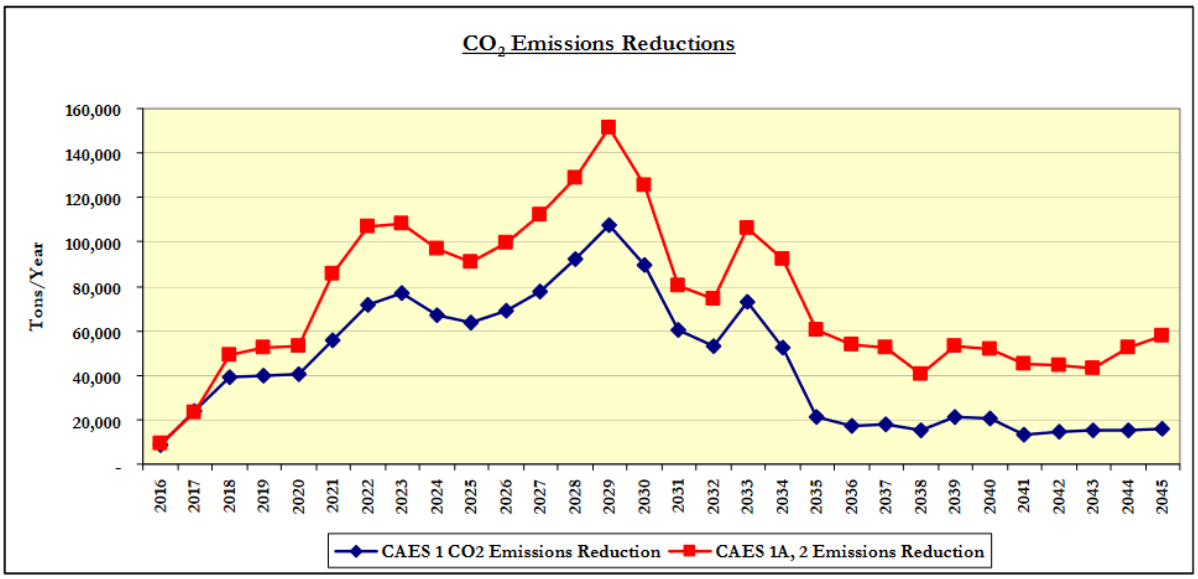

Figure 1A. Potential CO_2 Emission Reductions of proposed D-CAES facility on Seneca Lake[36].

Figure I-2: NYCA Summer Peak Forecasts – Coincident Peak, MW

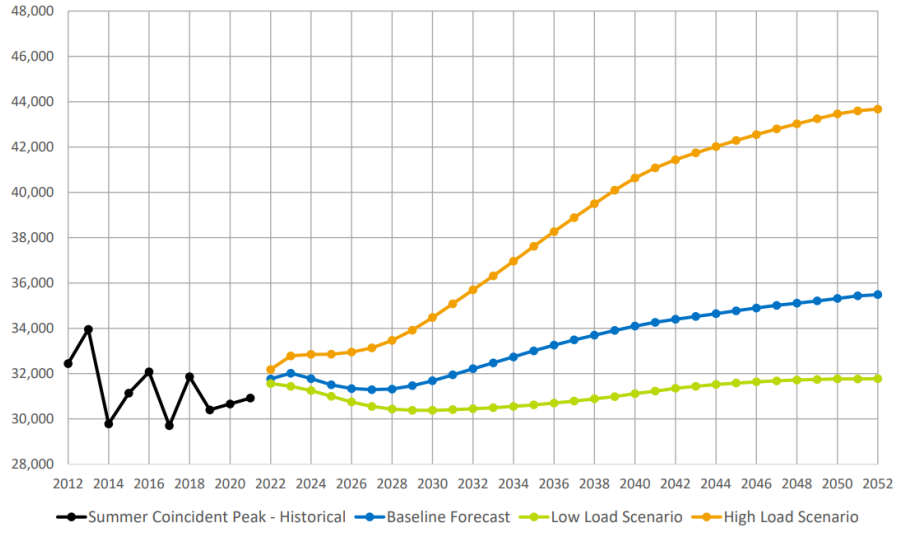

Figure I-3: NYCA Winter Peak Forecasts – Coincident Peak, MW

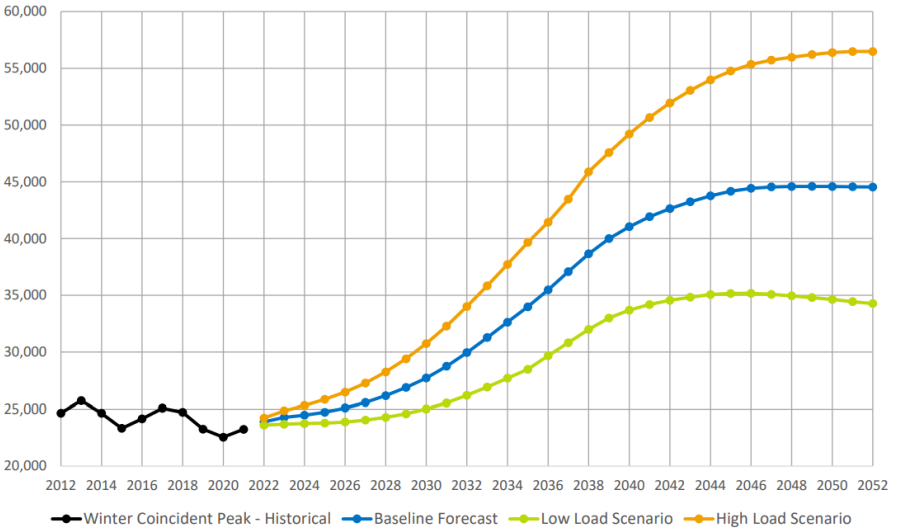

Figure A2. Forecast of peak energy demand in the summer and winter

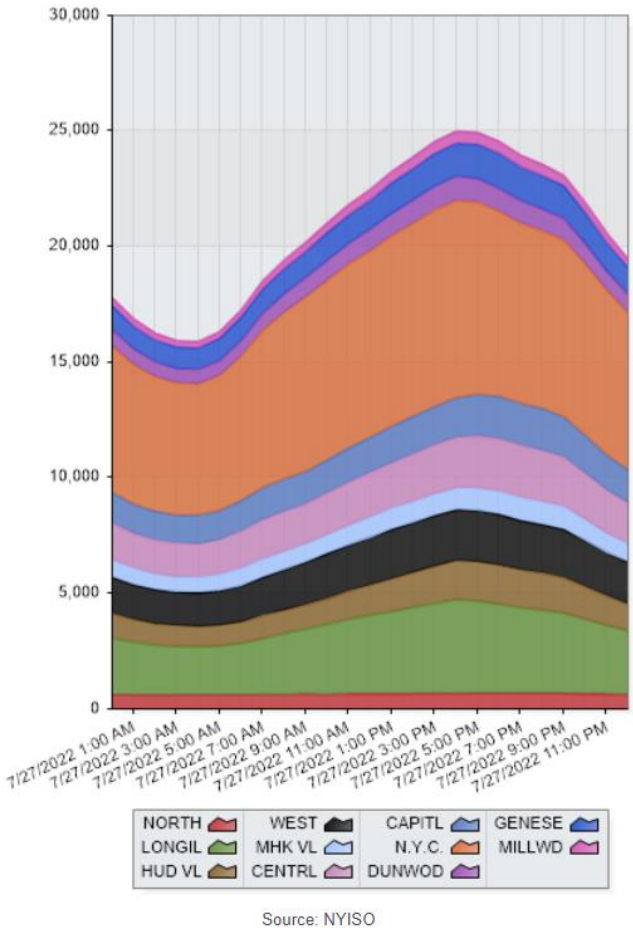

Figure A3. Actual Hourly Load for July 27, 2022[46].

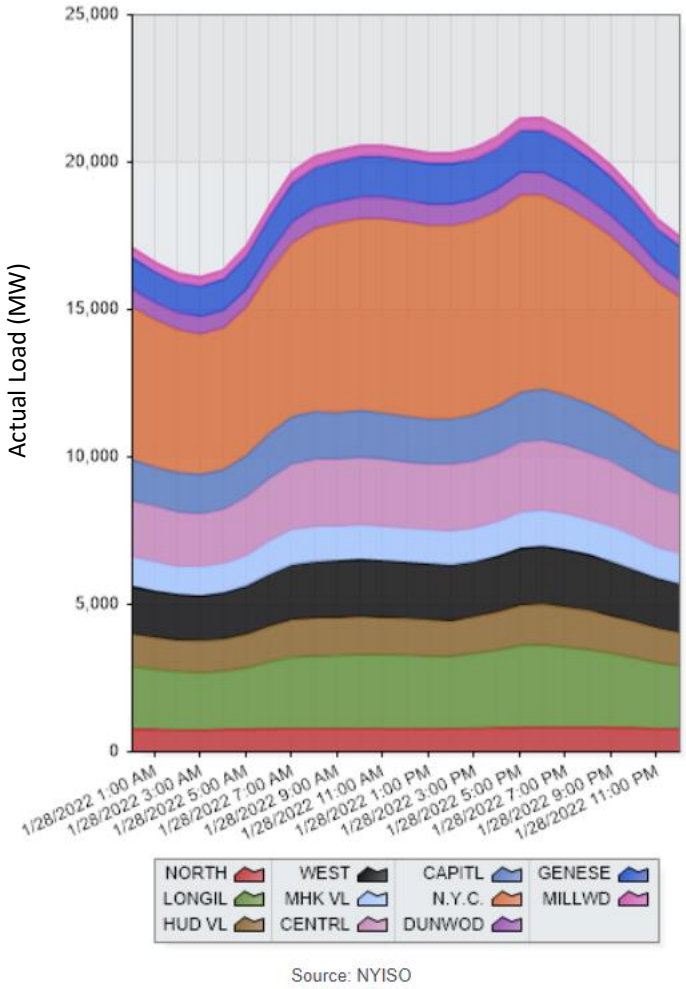

Figure A4. Actual Hourly Load for Jan 28, 2022[46].

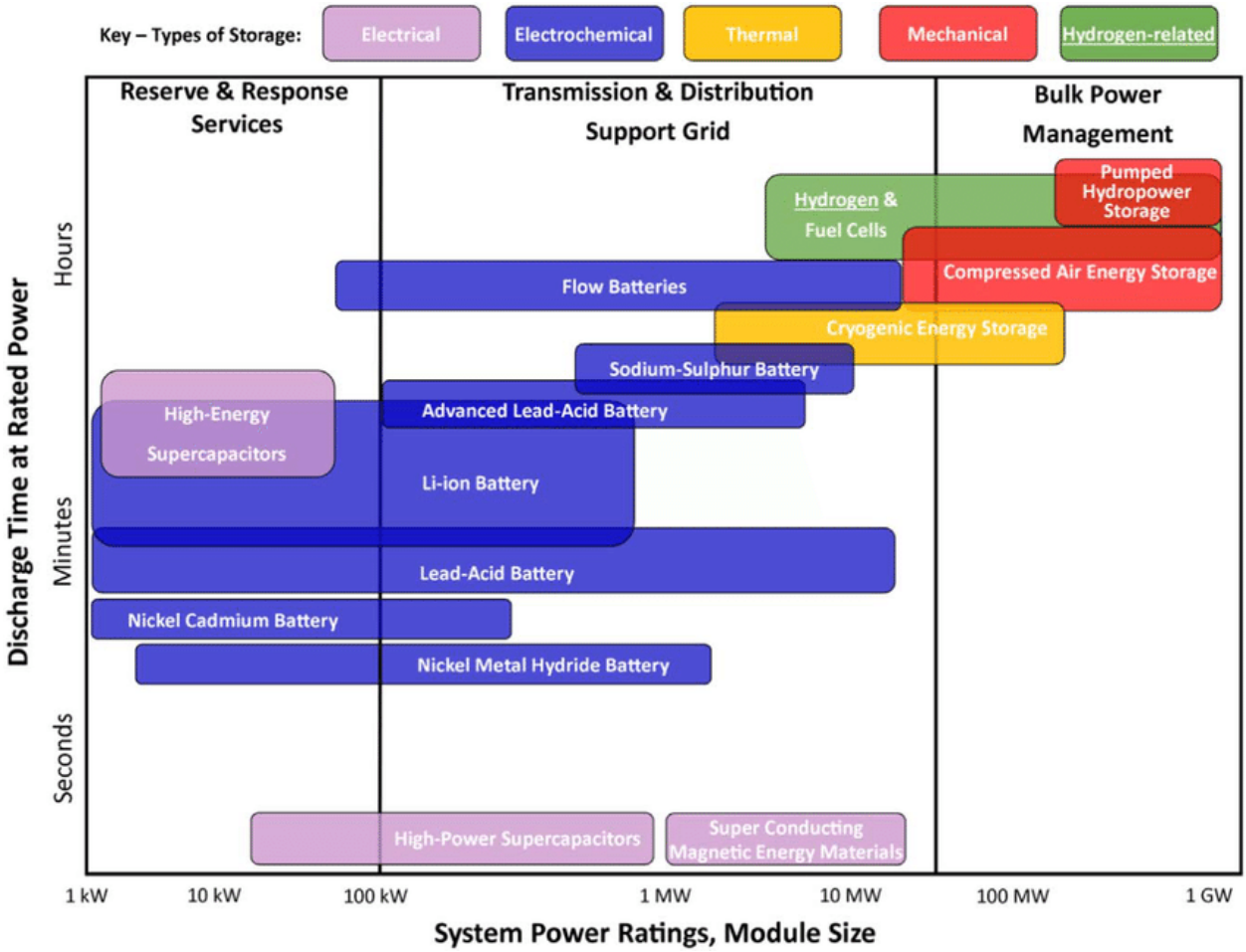

Figure A5. Comparison of energy storage technologies in rated power and discharge duration[49].